A modified low-rank Smith method for large-scale Lyapunov equations*

S. GUGERCIN[†], D.C. SORENSEN[‡], and A.C. ANTOULAS[†]

e-mail: {serkan,sorensen,aca}@rice.edu

August 13, 2002

Abstract

In this note we present a modified cyclic low-rank Smith method to compute low-rank approximations to solutions of Lyapunov equations arising from large-scale dynamical systems. Unlike the original cyclic low-rank Smith method introduced by Penzl in [19], the number of columns required by the modified method in the approximate solution does not necessarily increase at each step and is usually much lower than in the original cyclic low-rank Smith method. The modified method never requires more columns than the original one. Upper bounds are established for the errors of the low-rank approximate solutions and also for the errors in the resulting approximate Hankel singular values. Numerical results are given to verify the efficiency and accuracy of the new algorithm.

1 Introduction

Linear time invariant (LTI) systems

$$\mathbf{\Sigma}: \begin{cases} \dot{x}(t) &= Ax(t) + Bu(t) \\ y(t) &= Cx(t) + Du(t) \end{cases} \quad \Leftrightarrow \quad \mathbf{\Sigma} := \left(\begin{array}{c|c} A & B \\ \hline C & D \end{array} \right)$$

where $A \in \mathbb{R}^{n\times n}$, $B \in \mathbb{R}^{n\times m}$, $C \in \mathbb{R}^{p\times n}$, $D \in \mathbb{R}^{p\times m}$, arise frequently in many branches of engineering. Closely related to this system are two continuous-time Lyapunov equations:

$$A\mathcal{P} + \mathcal{P}A^T + BB^T = 0, \quad A^T\mathcal{Q} + \mathcal{Q}A + C^TC = 0 \tag{1.1}$$

Under the assumption that A is stable, it is well known that the above equations have unique symmetric positive semi-definite solutions $\mathcal{P}, \mathcal{Q} \in \mathbb{R}^{n\times n}$, called the *controllability* and *observability gramians*, respectively. In many applications, such as circuit simulation, or time dependent PDE control problems, n is quite large, while the number of inputs m and outputs p usually satisfy $m, p \ll n$. In these large scale settings, it is often desirable to approximate the given system with a much lower dimensional system

$$\mathbf{\Sigma}_r := \left(\begin{array}{c|c} A_r & B_r \\ \hline C_r & D_r \end{array} \right)$$

where $A_r \in \mathbb{R}^{r\times r}$, $B_r \in \mathbb{R}^{r\times m}$, $C_r \in \mathbb{R}^{p\times r}$, $D_r \in \mathbb{R}^{p\times m}$, with $r << n$. The problem of model reduction is to produce such a low dimensional system that will have approximately the same response (output) as the original system to any given input u.

*This work was supported in part by the NSF through Grants DMS-9972591, CCR-9988393 and ACI-0082645.

[†]Department of Electrical and Computer Engineering, MS 380, Rice University, Houston, Texas 77251-1892.

[‡]Department of Computational and Applied Mathematics, MS 134, Rice University, Houston, Texas 77251-1892.

Lyapunov matrix equations play a crucial role in the problem of model reduction. One of the most effective model reduction approaches called *balanced model reduction* [15], requires the solution of two Lyapunov equations to obtain controllability and observability gramians. A state space transformation is then derived to balance the system in the sense that the two gramians become diagonal and equal. In this new co-ordinate system, states that are difficult to reach are simultaneously difficult to observe. A stable reduced model of any specified order is obtained by truncating the system to retain the dominant portion of the gramians and thereby eliminate states that are both difficult to reach and difficult to observe.

The Bartels-Stewart [5] method as modified by Hammarling [11] is the standard direct method for the solution of Lyapunov equations of small to moderate size. This method requires the computation of a Schur decomposition, and thus is not appropriate for large scale problems. Iterative schemes have been developed including the Smith method [23], the sign-function method [21], the alternating direction implicit (ADI) iteration method [25], and the Smith(l) method [19]. Unfortunately, all of these methods compute the solution in dense form and hence require $\mathcal{O}(n^2)$ storage.

Many have observed that solutions to the Lyapunov equations associated with LTI systems have often low numerical rank (i.e. the eigenvalues decay rapidly). This phenomena is now better understood due to [4, 18]. One must take advantage of this low rank structure to obtain approximate solutions in low rank factored form. If the effective rank is $r \ll n$, then the storage is reduced from $\mathcal{O}(n^2)$ to $\mathcal{O}(nr)$. Such low rank schemes are the only existing methods that can effectively solve very large Lyapunov equations.

Most low rank methods [12], [13], [14] are Krylov subspace methods. Penzl [19] introduced two low-rank methods based on the ADI iteration, namely *low-rank ADI iteration* (LR-ADI), and *cyclic low-rank Smith method* (LR-Smith(l)). The latter method is a special case of the former where a small number of shifts are re-used in a cyclic manner.

The LR-ADI and LR-Smith(l) methods both compute a low-rank approximate square root factor of the solution. Unfortunately, the number of columns of these approximate solutions can be quite high. Indeed, when solving the Lyapunov equation, the LR-ADI and LR-Smith(l) add m and $m \times l$ columns respectively to the current solution at each step, where l is the number of shifts. For large n and especially for slowly converging iterations, the number of the columns of the solution can easily exceed manageable memory capacity.

In this paper, we introduce a modified LR-Smith(l) method that prevents the number of columns from increasing arbitrarily at each step. In fact, the modified method only requires the number of columns r needed to meet the pre-specified balanced truncation tolerance. Due to the rapid decay of the Hankel singular values, this r is usually quite small relative to n. Consequently the memory requirements are drastically reduced.

The rest of this paper is organized as follows: In Section 2, we review the model reduction problem and balanced truncation. Then Section 3 summarizes the following methods: (1) Alternating Direction Implicit (ADI) iteration, (2) Smith's Method, (3) Smith(l) Iteration, (4) low-rank ADI (LR-ADI) iteration, and (5) low-rank cyclic Smith(l) (LR-Smith(l)). Then in Section 4, we introduce the modified cyclic low-rank Smith iteration and present some convergence results. Section 5 gives the numerical results followed by conclusions in Section 6.

2 Model Reduction Problem

At present, there are a number of computational schemes for model reduction. Large scale problems offer additional challenges in storage and computational requirements over and above those of small to medium scale problems. In general, if we regard the two LTI systems as input-output maps:

$$\mathbf{\Sigma} : u \to y, \text{ and } \mathbf{\Sigma}_r : u \to \hat{y},$$

the goals are that **1**. the approximation error be *small*, and there exist a *global* error bound on $\|y - \hat{y}\|_2$, that **2**. system properties, like *stability*, *passivity*, be preserved, and that **3**. the procedure be *numerically stable* and *computationally efficient* with respect to storage and arithmetic operations.

Goals **1** and **2** are generally met through the underlying theory behind a reduction scheme. Meeting the third goal requires algorithmic development and implementation.

2.1 Balanced Truncation

One scheme that is well grounded in theory is *Balanced Truncation* as introduced by Moore [15]. The elegant approximation theory underlying this approach was developed by Glover [7]. Several researchers have recognized the importance of balanced truncation for model reduction because of it's theoretical properties. Computational schemes for small to medium scale problems already exist. However, the development of computational methods for the large scale setting is still an active area of research.

Let $\mathcal{P}$ and $\mathcal{Q}$ be the unique Hermitian positive definite solutions to equations (1.1). The square roots of the eigenvalues of the product $\mathcal{P}\mathcal{Q}$ are the singular values of the Hankel operator associated with $\mathbf{\Sigma}$ and are called Hankel singular values $\sigma_i(\mathbf{\Sigma})$ of the system $\mathbf{\Sigma}$:

$$\sigma_i(\mathbf{\Sigma}) = \sqrt{\lambda_i(\mathcal{P}\mathcal{Q})}.$$

In most cases, the eigenvalues of $\mathcal{P}, \mathcal{Q}$ as well as the Hankel singular values $\sigma_i(\Sigma)$ decay very rapidly. This phenomena is explained to a large extent in [4]. This observation motivates the development of low-rank approximate solution schemes and leads to model reduction by truncation.

Let $\mathcal{P} = UU^T$ and $\mathcal{Q} = LL^T$. U and L are called **square roots** of the gramians $\mathcal{P}$ and $\mathcal{Q}$ respectively. Let $U^T L = ZSY^T$ be the singular value decomposition (SVD), with $S = diag(\sigma_1, \sigma_2, \ldots, \sigma_n)$. Let $S_r = diag(\sigma_1, \sigma_2, \ldots, \sigma_r)$, $r < n$ and define

$$W_r = LY_r S_r^{-1/2} \quad \text{and} \quad V_r = UZ_r S_r^{-1/2}. \tag{2.1}$$

where Z_r and Y_r are composed of the leading r columns of Z and Y respectively. It is easy to check that $W_r^T V_r = I_r$ and hence that $V_r W_r^T$ is an oblique projector. We obtain a reduced model of order r by putting

$$A_r = W_r^T A V_r, \;\; B_r = W_r^T B, \;\; C_r = CV_r.$$

Noting that $\mathcal{P}W_r = V_r S_r$ and $\mathcal{Q}V_r = W_r S_r$ gives

$$\begin{aligned} W_r^T(A\mathcal{P} + \mathcal{P}A^T + BB^T)W_r &= A_r S_r + S_r A_r^T + B_r B_r^T \\ V_r^T(A^T\mathcal{Q} + \mathcal{Q}A + C^T C)V_r &= A_r^T S_r + S_r A_r + C_r^T C_r \end{aligned}$$

Thus, the reduced model is balanced and asymptotically stable (due to the Lyapunov inertia theorem) for any $r \le n$. Moreover, the formulas above provide a numerically stable scheme for computing the reduced order model based on a numerically stable scheme for computing the square roots U and L directly in upper triangular and lower triangular form respectively. It is important to truncate Z, S, Y to Z_r, S_r, Y_r prior to forming W_r or V_r. It is also important to avoid formulas involving inversion of L or U as these matrices are typically ill-conditioned due to the decay of the eigenvalues of the gramians.

The reduced system $\mathbf{\Sigma}_r = \left[\begin{array}{c|c} A_r & B_r \\ \hline C_r & D_r \end{array}\right]$, of order r has the following properties: A_r is stable and the $\mathcal{H}_\infty$ norm of the error system satisfies

$$\|\mathbf{\Sigma} - \mathbf{\Sigma}_r\|_\infty \le 2(\sigma_{r+1} + \cdots + \sigma_n). \tag{2.2}$$

For details, see [1].

3 ADI, Smith, and Cyclic Smith(l) Iterations

For high order systems (large n), the balanced truncation method described in Section 2 requires the solution to Lyapunov equations of order n. Moreover, as previously explained, $\mathcal{P}$ and $\mathcal{Q}$ are often found to have *numerically* low-rank compared to n. This *low-rank phenomenon* leads to the idea of approximating the gramians with low rank approximate gramians.

In the following discussion, we shall focus on the approximate solution of a single Lyapunov equation

$$A\mathcal{P} + \mathcal{P}A^T + BB^T = 0, \tag{3.1}$$

where $A \in \mathbb{R}^{n\times n}$ is stable and diagonalizable, and $B \in \mathbb{R}^{n\times m}$. The ideas developed, apply equally well to the computation of the observability gramian. In this section we first briefly review the ADI, Smith and Smith(l) methods in Section 3.1, Section 3.2 and Section 3.3 respectively. These are iterative methods for computing the solution $\mathcal{P}$. Section 3.4 summarizes LR-ADI and LR-Smith(l) iterations, first introduced in [19] which yield low-rank approximations to $\mathcal{P}$ followed by a concise implementation of multi-shift Smith iteration in Section 3.5. Then we present some convergence results for the LR-Smith(l) iteration in Section 3.6. In all of these methods the idea is to transform a continuous time Lyapunov equation (3.1) into a discrete time Stein equation using spectral transformations of type $\omega(\lambda) = \frac{\mu^* - \lambda}{\mu + \lambda}$ where $\mu \in \mathbb{C}_-$ (the open left half-plane). Note that ω is a bilinear transformation mapping the open left half-plane onto the open unit disk with $\omega(\infty) = -1$. The parameter μ is the *shift*.

In the ADI method, one uses a different shift at each step and obtains a series of Stein equations which can be solved iteratively. Smith's method which uses a single shift parameter is a special case of the ADI iteration. The solution of the resulting Stein equation can be computed as an infinite sum. The Smith(l) method is also a special case of the ADI iteration where l shifts are used in a cyclic manner. Like the Smith iteration, a discrete Stein equation is obtained. In case of a single shift, the resulting discrete time system has the same number of inputs and outputs as the continuous time system. On the other hand, when l multiple shifts are used, the number of inputs and outputs is increased l times.

The original versions of the ADI, Smith, and Smith(l) methods form and store the entire dense solution $\mathcal{P}$ explicitly and this requires extensive memory. The observation that $\mathcal{P}$ is of numerically low-rank compared to n leads to the low-rank iterations LR-ADI and LR-Smith(l) where only low-rank approximate factorizations of $\mathcal{P}$ are computed and stored reducing memory requirements considerably.

3.1 The ADI Iteration

The alternating direction implicit (ADI) iteration was first introduced by Peaceman and Rachford [17] to solve linear systems arising from the discretizations of elliptic boundary value problems. In general, the ADI iteration is used to solve the linear systems of the form

$$My = b$$

where M is symmetric positive definite and can be split into the sum of two symmetric positive definite matrices $M = M_1 + M_2$ for which the following iteration is efficient.

$$\begin{aligned} y_0 &= 0, \\ (M_1 + \mu_j I)y_{j-1/2} &= b - (M_2 - \mu_j I)y_{j-1}, \\ (M_2 + \eta_j I)y_j &= b - (M_1 - \eta_j I)y_{j-1/2}, \text{ for } j = 1, 2, \cdots, J. \end{aligned}$$

The ADI shift parameters μ_j and η_j are determined from spectral bounds on M_1 and M_2 to increase the convergence rate. When M_1 and M_2 commute, this is classified as a "model problem".

One should notice that (3.1) is a model ADI problem in which there is a linear system with the sum of two commuting operators acting on the unknown $\mathcal{P}$, which is a matrix in this case. Therefore, the iterates $\mathcal{P}_i^A$ of the ADI iteration are obtained through the iteration steps

$$\begin{aligned}(A+\mu_i I)\mathcal{P}_{i-1/2}^A &= -BB^T - \mathcal{P}_{i-1}^A(A^T-\mu_i I)\\ (A+\mu_i I)\mathcal{P}_i^A &= -BB^T - (\mathcal{P}_{i-1/2}^A)^*(A^T-\mu_i I)\end{aligned}$$

where $\mathcal{P}_0^A = 0$ and the shift parameters $\{\mu_1,\mu_2,\mu_3,\dots\}$ are elements of $\mathbb{C}_-$ (here $*$ denotes complex conjugation followed by transposition). These two equations are equivalent to the following single iteration step:

$$\mathcal{P}_i^A = (A-\mu_i^* I)(A+\mu_i I)^{-1}\mathcal{P}_{i-1}^A[(A-\mu_i^* I)(A+\mu_i I)^{-1}]^* - 2\rho_i(A+\mu_i I)^{-1}BB^T(A+\mu_i I)^{-*}, \tag{3.2}$$

where $\rho_i = \mathrm{Real}(\mu_i)$. Note that if $\mathcal{P}_{i-1}$ is Hermitian positive semi-definite, then so is $\mathcal{P}_i$.

The spectral radius $\rho_{_{ADI}} = \rho\left(\prod_{i=1}^{l}(A-\mu_i^* I)(A+\mu_i I)^{-1}\right)$ determines the rate of convergence where l is the number of shifts used. The minimization of $\rho_{_{ADI}}$ with respect to shift parameters μ_i is called the ADI minimax problem:

$$\{\mu_1,\mu_2,\dots,\mu_l\} = \arg \min_{\{\mu_1,\mu_2,\dots,\mu_l\}\in\mathbb{C}_-} \max_{\lambda\in\sigma(A)} \frac{|\,(\lambda-\mu_1^*)\dots(\lambda-\mu_l^*)\,|}{|\,(\lambda+\mu_1)\dots(\lambda+\mu_l)\,|}.$$

We refer the reader to [6], [22], and [26] for contributions to the solution of the ADI minmax problem. It can be shown that if A is diagonalizable, the l^{th} iterate satisfies the inequality

$$\|\mathcal{P}-\mathcal{P}_l^A\|_F \le \|X\|^2\|X^{-1}\|^2\,\rho_{_{ADI}}^2\,\|\mathcal{P}\|_F$$

where X is the matrix of eigenvectors of A.

The schemes that follow are quite similar to the ADI method in terms of the basic computational operations involving application of these spectral transformations. We wish to emphasize that each individual shift μ_i requires a sparse direct factorization of $(A+\mu_i I)$ and each application of $(A+\mu_i I)^{-1}$ requires triangular solves from that factorization. Moreover, these operations have to be done in complex arithmetic if complex shifts are used. To keep the solution $\mathcal{P}$ in real arithmetic, complex conjugate pairs of shifts have to be applied one followed immediately by the other. However, even with this, one would have to form $(A+\mu_i I)(A+\mu_i^* I) = A^2 + 2\rho_i A + |\mu_i|^2 I$ in order to keep the factorizations in real arithmetic. This matrix squaring would most likely have an adverse effect on sparsity. In the sequel, we wish to avoid the additional detail required to discuss complex shifts. As just shown, all of the operations can be made valid for complex shifts if necessary. However, for the reasons just given, complex shifts are not very practical and generally do not improve convergence rates over real shifts. Therefore, we will restrict our attention to real shifts for the remainder of this discussion.

3.2 Smith's Method

For every real scalar $\mu < 0$, (3.1) is equivalent to

$$\mathcal{P} = (A-\mu I)(A+\mu I)^{-1}\mathcal{P}(A+\mu I)^{-T}(A-\mu I)^T - 2\mu(A+\mu I)^{-1}BB^T(A^T+\mu I)^{-1}.$$

Define

$$A_\mu := (A-\mu I)(A+\mu I)^{-1},\ B_\mu := (A+\mu I)^{-1}B. \tag{3.3}$$

Then one obtains the Stein equation

$$\mathcal{P} = A_\mu \mathcal{P} A_\mu^T - 2\mu B_\mu B_\mu^T. \tag{3.4}$$

Hence using the bilinear transformation $\omega = \frac{\mu-\lambda}{\mu+\lambda}$, the problem has been transformed into discrete time where the Stein equation (3.4) has the same solution as the continuous time Lyapunov equation (3.1). Since A is stable, $\rho(A_\mu) < 1$ and the sequence $\{\mathcal{P}_i^S\}_{i=0}^{\infty}$ generated by the iteration

$$\mathcal{P}_1^S = -2\mu B_\mu B_\mu^T \text{ and } \mathcal{P}_{j+1}^S = A_\mu \mathcal{P}_j^S A_\mu^T + \mathcal{P}_1^S$$

converges to the solution $\mathcal{P}$. Thus, the Smith iterates can be written as

$$\mathcal{P}_k^S = -2\mu \sum_{j=0}^{k-1} A_\mu^j B_\mu B_\mu^T (A_\mu^j)^T. \tag{3.5}$$

If all of the shifts in the ADI method are constant ($\mu_j = \mu,\ j = 1, 2, \ldots$) then the ADI iteration reduces to the Smith method. Generally, the convergence of the Smith method is slower than ADI. An accelerated version, the so called squared Smith method, has been proposed in [19] to improve the convergence.

3.3 Smith-l Iteration

In [19], computational experience would indicate that ADI with a single shift (Smith's method) converges very slowly, while a moderate increase in the number of shifts l accelerates the convergence nicely. However, it is also observed that the speed of convergence is hardly improved by a further increase of l; see Table 2.1 in [19]. These observations lead to the idea of cyclic Smith(l) iteration, a special case of ADI where l different shifts are used in a cyclic manner, i.e. $\mu_{i+jl} = \mu_i$ for $j = 1, 2, \cdots$. It readily follows that the Smith(l) iterates are generated by

$$\mathcal{P}_k^{Sl} = \sum_{j=0}^{k-1} A_d^j T (A_d^j)^T. \tag{3.6}$$

where

$$A_d = \prod_{i=1}^{l} (A - \mu_i I)(A + \mu_i I)^{-1} \qquad \text{and} \qquad T = P_l^A \tag{3.7}$$

i.e. T is the l^{th} ADI iterate with shifts $\{\mu_1, \cdots, \mu_l\}$. As in Smith's methods, $\mathcal{P} - A_d \mathcal{P} A_d^T = T$ is equivalent to (3.1) where A_d and T are defined in (3.7).

3.4 LR-ADI and LR-Smith(l) Iterations

Since the solution $\mathcal{P}$ is explicitly computed, the ADI, Smith and Smith(l) iterations outlined above, have the storage requirement $\mathcal{O}(n^2)$. One should notice that in many cases the storage requirement is the limiting factor rather than the amount of computation. Low-rank methods are the only existing methods that can effectively solve large scale Lyapunov equations. Instead of explicitly forming the solution $\mathcal{P}$, the low-rank methods compute and store the low-rank approximate square root factors reducing the storage requirement to $\mathcal{O}(nr)$ where r is the numerical rank of $\mathcal{P}$.

The key idea in the low-rank versions of Smith(l) and ADI methods is to write

$$\mathcal{P}_i^{Sl} = Z_i^{Sl} (Z_i^{Sl})^T \quad \text{and} \quad \mathcal{P}_i^A = Z_i^A (Z_i^A)^T. \tag{3.8}$$

This is always possible since the iterates P_i^{Sl} and $\mathcal{P}_i^A$ can be shown recursively to be positive definite and symmetric.

The low-rank ADI (LR-ADI) is based on (3.2). Using (3.8), (3.2) can be reformulated in terms of the low-rank factors Z_i^A as

$$Z_i^A = [\,(A-\mu_i I)(A+\mu_i I)^{-1}Z_{i-1}^A \quad \sqrt{-2\mu_i}(A+\mu_i I)^{-1}B\,] \tag{3.9}$$

with

$$Z_1^A = \sqrt{-2\mu_1}(A+\mu_1 I)^{-1}B$$

This method is of interest if a sequence $\{\mu_i\}_{i=1}^{\infty}$ of different shifts is available. When the number of shift parameters is limited, the cyclic low-rank Smith method (LR-Smith(l)) is a more efficient alternative to the LR-ADI. The methods consists of two steps. First the iterate Z_1^{Sl} is obtained by an l step low-rank ADI iteration; i.e. $X_l^A = Z_l^A(Z_l^A)^T$ is the low-rank l step ADI iteration. Then, the LR-Smith(l) is initialized by

$$Z_1^{Sl} = B_d = Z_l^A \tag{3.10}$$

followed by the actual LR-Smith(l) iteration:

$$\begin{aligned} Z^{(i+1)} &= A_d Z^{(i)} \\ Z_{i+1}^{Sl} &= [\,Z_i^{Sl} \;\; Z^{(i+1)}\,] \end{aligned} \tag{3.11}$$

where A_d is defined in (3.7). It then follows that

$$Z_k^{Sl} = [\,B_d \;\; A_dB_d \;\; A_d^2B_d \;\; \cdots \;\; A_d^{k-1}B_d\,]. \tag{3.12}$$

One should notice that while a k step LR-ADI iteration requires k matrix factorizations, a k step LR-Smith(l) iteration computes only l matrix factorization. If the shifts $\{\mu_1, \cdots, \mu_l\}$ are used in a cyclic manner, the cyclic LR-Smith(l) iteration is equivalent to LR-ADI iteration.

We note that at the i^{th} step, Z_i^A and Z_i^{Sl} has $m \times i$ and $m \times l \times i$ columns respectively; i.e. at each iteration the number of columns is increased by m for the LR-ADI and by $m \times l$ for the LR-Smith(l) iterations. Hence when m is large or the convergence is slow, i.e. $\rho(A_d)$ is close to 1, the number of columns of Z_k^A and Z_k^{Sl} will easily reach unmanageable levels of memory requirements, and these two methods will fail. Slow convergence is observed when the eigenvalues of A are spread out in the complex plane and this will be the case for most of the structural systems, see [10]. In Section 4 we introduce a modified LR-Smith(l) iteration which will remedy this problem and retain the low-rank structure.

Remark 3.1 **1**. A system theoretic interpretation of using l cyclic shifts (the Smith(l) iteration) is that we embed the continuous time system $\mathbf{\Sigma} = \left(\begin{array}{c|c} A & B \\ \hline C & D \end{array}\right)$ which has order n, m input and p outputs into a discrete time system $\mathbf{\Sigma}_d = \left(\begin{array}{c|c} A_d & B_d \\ \hline C_d & D_d \end{array}\right)$ which has order n, lm inputs and lp outputs; and has the same controllability and observability gramians $\mathcal{P}$ and $\mathcal{Q}$. Therefore at the cost of increasing the number of inputs and outputs, we reduce the spectral radius $\rho(A_d)$ and hence increase the convergence.

2. Assume that we know all the eigenvalues of A and the system $\mathbf{\Sigma} = \left(\begin{array}{c|c} A & B \\ \hline C & D \end{array}\right)$ is single input single output. Then choosing $\mu_i = \lambda_i(A)$ for $i = 1, \cdots, n$ results in

$$A_d = 0 \qquad \text{and} \qquad \mathcal{P} = \mathcal{P}_1^{Sl} = T = \mathcal{P}_l^A$$

In other words, the exact solution $\mathcal{P}$ of (3.1) is obtained at the first step. The resulting discrete time system has n inputs, and n outputs.

3.5 A Multi-shift Smith Iteration

If the LR-Smith(l) iteration is implemented in the fashion presented above, one is obliged to either store or re-compute l factorizations of the shifted matrices $A - \mu_{i+jl}I$.

In the following, we explain how to re-arrange this computation so that the individual factorizations may be discarded after use. A factorization corresponding to a new shift may overwrite the previous one.

We first note that

$$\mathcal{P} - \mathcal{P}_k = -2\mu \sum_{j=k}^{\infty} A_\mu^j B_\mu B_\mu^T (A_\mu^T)^j = A_\mu^k \mathcal{P} (A_\mu^T)^k \geq 0.$$

Moreover, since A commutes with A_μ we have

$$\begin{aligned} A\mathcal{P}_k + \mathcal{P}_k A^T + BB^T &= A(\mathcal{P}_k - P) + (\mathcal{P}_k - \mathcal{P})A^T \\ &= -[AA_\mu^k \mathcal{P}(A_\mu^T)^k + A_\mu^k \mathcal{P}(A_\mu^T)^k A^T] \\ &= -A_\mu^k [A\mathcal{P} + \mathcal{P}A^T](A_\mu^T)^k \\ &= A_\mu^k BB^T (A_\mu^T)^k \geq 0. \end{aligned}$$

From this expression, we see that

$$\begin{aligned} 0 &= A(\mathcal{P} - \mathcal{P}_k) + (\mathcal{P} - \mathcal{P}_k)A^T + A\mathcal{P}_k + \mathcal{P}_k A^T + BB^T \\ &= A(\mathcal{P} - \mathcal{P}_k) + (\mathcal{P} - \mathcal{P}_k)A^T + A_\mu^k BB^T (A_\mu^T)^k. \end{aligned}$$

Let $B_{(\mu,\eta)} = (A + \eta I)^{-1} A_\mu^k B$. Then, for any other shift $\eta < 0$ we have

$$\mathcal{P} - \mathcal{P}_k = A_\eta (\mathcal{P} - \mathcal{P}_k) A_\eta^T - 2\eta B_{(\mu,\eta)} B_{(\mu,\eta)}^T.$$

In general, define $B_{(j)} := A_{\mu_{j-1}}^{k_{j-1}} B_{(j-1)}$ and let $\mathcal{P}_{(j)} := \sum_{i=0}^{k_j - 1} A_{\mu_j}^i B_{(j)} B_{(j)}^T (A_{\mu_j}^T)^i$. Let $\mathcal{P}_k = \mathcal{P}_{(1)} + \mathcal{P}_{(2)} + \ldots + \mathcal{P}_{(k)}$. Then

$$A(\mathcal{P} - \mathcal{P}_k) + (\mathcal{P} - \mathcal{P}_k)A^T + B_{(k+1)} B_{(k+1)}^T = 0.$$

This derivation might suggest that a multishift method would be very complicated to program. However, a very concise implementation is possible as the following code will illustrate.

```
Bm = B;
R = [];
for j = 1:kshifts,
   mu = u(j);
   rho = sqrt(2*mu);
   Bm = ((A - mu*eye(n))\Bm);
   R = [R rho*Bm];
   for j = 1:ksteps,
      Bm = (A + mu*eye(n))*((A - mu*eye(n))\Bm);
      R = [R rho*Bm];
   end
   Bm = (A + mu*eye(n))*Bm;
end
[V,S,Q] = svd(R,0);
R = V*S;
```

3.6 Convergence Results for the Cyclic LR-Smith(l) iteration

In this section we shall establish some fundamental convergence results for the Cyclic LR-Smith(l) iteration.

Let $\{\mu_1, \cdots, \mu_l\}$ be the l shifts used in the LR-Smith(l) iteration. As stated in Section 3.2, (3.1) is equivalent to the Stein equation

$$\mathcal{P} - A_d \mathcal{P} A_d^T + B_d B_d^T = 0 \tag{3.13}$$

where A_d, and B_d are defined in (3.7) and (3.10) respectively. Let Z_k^{Sl} be given by (3.12). Similarly to Z_k^{Sl} and B_d, let C_d and Y_k^{Sl} be obtained by the following l step low-rank ADI iteration as follows:

$$Y_i^A = [\ (A^T - \mu_i I)(A^T + \mu_i I)^{-1} Y_{i-1}^A \quad \sqrt{-2\mu_i}(A^T + \mu_i I)^{-1} C^T\ ]$$

$$\text{with } Y_1^A = \sqrt{-2\mu_1}(A^T + \mu_1 I)^{-1} C^T \qquad \text{and}$$

$$\begin{aligned} C_d &= (Y_l^A)^T, & (3.14)\\ Y_k^{Sl} &= [\ C_d^T \ \ A_d^T C_d^T \ \ (A_d^T)^2 C_d^T \ \cdots \ (A_d^{k-1})^T C_d^T\ ] & (3.15)\end{aligned}$$

Denote by $\mathcal{P}_k^{Sl}$ and $\mathcal{Q}_k^{Sl}$ the k step LR-Smith(l) iterates to $\mathcal{P}$ and $\mathcal{Q}$ respectively, i.e. $\mathcal{P}_k^{Sl} = Z_k^{Sl}(Z_k^{Sl})^T$ and $\mathcal{Q}_k^{Sl} = Y_k^{Sl}(Y_k^{Sl})^T$. One should notice that the errors are $E_{kp} = \mathcal{P} - \mathcal{P}_k^{Sl} \geq 0$ and $E_{kq} = \mathcal{Q} - \mathcal{Q}_k^{Sl} \geq 0$. We will use the trace as a norm of the errors. This leads to the following proposition:

Proposition 3.1 *Let E_{kp} and E_{kq} be defined as above, and $A = X(\Lambda)X^{-1}$ be the eigenvalue decomposition of A. The k step LR-Smith(l) iterates satisfy*

$$\begin{aligned} 0 &\leq \mathbf{Tr}\,(E_{kp}) = \mathbf{Tr}\,(\mathcal{P} - \mathcal{P}_k^{Sl}) \leq K\,m\,l\,(\rho(A_d))^{2k}\,\mathbf{Tr}\,(\mathcal{P}) & (3.16)\\ 0 &\leq \mathbf{Tr}\,(E_{kq}) = \mathbf{Tr}\,(\mathcal{Q} - \mathcal{Q}_k^{Sl}) \leq K\,p\,l\,(\rho(A_d))^{2k}\,\mathbf{Tr}\,(\mathcal{Q}) & (3.17)\end{aligned}$$

where

$$K = \kappa(X)^2, \tag{3.18}$$

where $\kappa(X)$ denotes the condition number of X.

Proof: We will prove the result for E_{kp} only. The lower bound is obvious from the fact that $E_{kp} \geq 0$. To prove the lower bound, we proceed as follows:

$$\begin{aligned} \mathbf{Tr}\,(E_{kp}) &= \mathbf{Tr}\left(\sum_{i=k}^{\infty} A_d^i B_d B_d^T (A_d^T)^i\right) = \sum_{i=k}^{\infty} \|A_d^i B_d\|_F^2 \\ &\leq m\,l \sum_{i=k}^{\infty} \|A_d^i B_d\|_2^2 \leq K\,m\,l\,(\rho(A_d))^{2k} \sum_{i=0}^{\infty} \|A_d^i B_d\|_2^2 \\ &\leq K\,m\,l\,(\rho(A_d))^{2k}\,\mathbf{Tr}\,(\mathcal{P}) \end{aligned}$$

The result for E_{kq} follows similarly. ■

Let σ_i and $\hat{\sigma}_i$ denote Hankel singular values resulting from the full-rank exact gramians and the low-rank approximate grammian respectively, i.e.

$$\sigma_i^2 = \lambda_i(\mathcal{P}\mathcal{Q}) \quad \text{and} \quad \hat{\sigma}_i^2 = \lambda_i(\mathcal{P}_k^{Sl}\mathcal{Q}_k^{Sl}). \tag{3.19}$$

Corollary 3.1 *Let σ_i and $\hat{\sigma}_i$ be given by (3.19). Define $\hat{n} = kl\min(m,p)$. Then,*

$$0 \;\leq\; \sum_{i=1}^{n}\sigma_i^2 - \sum_{i=1}^{\hat{n}}\hat{\sigma}_i^2 \;\leq\; K\,l\,(\rho(A_d))^{2k}\Big(K\,\min(m,p)(\rho(A_d))^{2k}\mathbf{Tr}\,(\mathcal{P})\mathbf{Tr}\,(\mathcal{Q}) + m\,\mathbf{Tr}\,(\mathcal{P})\sum_{i=0}^{k-1}\|C_dA_d^j\|_2^2 + p\,\mathbf{Tr}\,(\mathcal{Q})\sum_{i=0}^{k-1}\|A_d^jB_d\|_2^2\Big) \tag{3.20}$$

where K is as defined in (3.18).

Proof: From the definitions of σ_i and $\hat{\sigma}_i$ in (3.19) follow

$$\sum_{i=1}^{n}\sigma_i^2 - \sum_{i=1}^{\hat{n}}\hat{\sigma}_i^2 = \mathbf{Tr}\,(\mathcal{P}\mathcal{Q}) - \mathbf{Tr}\,(\mathcal{P}_k^{Sl}\mathcal{Q}_k^{Sl}).$$

Then, some simple manipulations lead to

$$\sum_{i=1}^{n}\sigma_i^2 - \sum_{i=1}^{\hat{n}}\hat{\sigma}_i^2 \;=\; \underbrace{\mathbf{Tr}\left(\sum_{i=0}^{k-1}\mathcal{M}_i\sum_{j=k}^{\infty}\mathcal{N}_i\right)}_{\eta_1} + \underbrace{\mathbf{Tr}\left(\sum_{i=k}^{\infty}\mathcal{M}_i\sum_{j=0}^{k-1}\mathcal{N}_i\right)}_{\eta_2} + \underbrace{\mathbf{Tr}\left(\sum_{i=k}^{\infty}\mathcal{M}_i\sum_{j=k}^{\infty}\mathcal{N}_i\right)}_{\eta_3}$$

where $\mathcal{M}_i := A_d^iB_dB_d^T(A_d^T)^i$ and $\mathcal{N}_i := (A_d^T)^jC_d^TC_dA_d^j$. We start by examining η_3:

$$\eta_3 \;=\; \mathbf{Tr}\left(\sum_{i=k}^{\infty}A_d^iB_dB_d^T(A_d^T)^i\sum_{j=k}^{\infty}(A_d^T)^jC_d^TC_dA_d^j\right) = \sum_{i=k}^{\infty}\sum_{j=k}^{\infty}\|C_dA_d^{(i+j)}B_d\|_F^2 \;\geq\; 0$$

Hence we simply obtain

$$\begin{aligned}
0 \;\leq\; \eta_3 \;&\leq\; l\,\min(m,p)\sum_{i=k}^{\infty}\|A_d^iB_d\|_2^2\sum_{j=k}^{\infty}\|C_dA_d^j\|_2^2 \;\Rightarrow\\
0 \;\leq\; \eta_3 \;&\leq\; K^2\,l\,\min(m,p)\,(\rho(A_d))^{4k}\sum_{i=0}^{\infty}\|A_d^iB_d\|_2^2\sum_{j=0}^{\infty}\|C_dA_d^j\|_2^2 \;\Rightarrow\\
0 \;\leq\; \eta_3 \;&\leq\; K^2\,l\,\min(m,p)\;(\rho(A_d))^{4k}\,\mathbf{Tr}\,(\mathcal{P})\mathbf{Tr}\,(\mathcal{Q})
\end{aligned}$$

A similar argument yields

$$\begin{aligned}
0 \;\leq\; \eta_1 \;&\leq\; K\,l\,m\;(\rho(A_d))^{2k}\,\mathbf{Tr}\,(\mathcal{P})\sum_{i=0}^{k-1}\|C_dA_d^j\|_2^2\\
0 \;\leq\; \eta_2 \;&\leq\; K\,l\,p\;(\rho(A_d))^{2k}\,\mathbf{Tr}\,(\mathcal{Q})\sum_{i=0}^{k-1}\|A_d^jB_d\|_2^2
\end{aligned}$$

Hence, the error in the Hankel singular values satisfies

$$0 \;\leq\; \sum_{i=1}^{n}\sigma_i^2 - \sum_{i=1}^{\hat{n}}\hat{\sigma}_i^2 = \eta_1 + \eta_2 + \eta_3$$

which gives the desired result. ■

Remark 3.2 *One should notice that the above error bounds critically depend on* $\rho(A_d)$ *and* K. *Hence when* $\rho(A_d)$ *is almost* 1 *and/or* A *is highly non-normal, the above error bound may be very pessimistic. These facts will be illustrated by means of numerical examples in Section 5.*

Remark 3.3 *In obtaining the above error bounds, we have assumed that* A *is diagonalizable. The results can be extended to the general case where* A *contains Jordan blocks. In that case, one should use the Schur decomposition of* A *instead of the eigenvalue decomposition. Let* $A = W(\Lambda + N)W^T$ *be the Schur decomposition of* A *where* $WW^T = I$, Λ *is diagonal and* N *is strictly upper triangular. Then in the above results, the term* $\rho(A_d)$ *should replaced by* $(\rho(A_d) + \epsilon)$ *where* $\epsilon > 0$ *with* $\rho(A_d) + \epsilon < 1$ *and* K *should be replaced by* $K_\epsilon = \left(\frac{\|N\|_F}{\epsilon}\right)^{2(n-1)}$. *Notice that such an* ϵ *always exists. This bound is quite pessimistic and hence is of little practical value. Hence, we omit the derivation.*

4 The Modified LR-Smith(l) Iteration

As already mentioned in Section 3.4, the LR-Smith(l) iteration has the drawback that when applied to the Lyapunov equation(3.1), the number of columns of the approximate square-root is increased by $m \times l$ at each step, where m is the number of inputs and l is the number of cyclic shifts applied. Hence in case of large m and slow convergence, this will cause storage problems. In Example-1, Section 5.1, a system of order 120 is given that describes the dynamics of the tracking mechanism of a portable CD player. The LR-Smith(l) method is slow to converge even for a large relative error tolerance of 3.95×10^{-3} in the computed gramians. Seventy LR-Smith(l) iteration steps are needed, resulting in a square root factor with 70 columns. However, its numerical rank is only 42. In light of these observations, we propose n Section 4.1 a modified LR-Smith(l) iteration so that the number of columns in the low-rank square root factor does not increase unnecessarily at each step. The idea is to compute the singular value decomposition of the iterate at each step and, given a tolerance τ, to replace the iterate with its best low-rank approximation. However, instead of recomputing the SVD, it is updated after each step to include the new information and then truncated to retain only those singular values that lie above the specified tolerance. Computational details of the algorithm are presented in the next section and followed by a discussion of the convergence properties in Section 4.2

4.1 The Proposed Algorithm

Again, consider the Lyapunov equation (3.1) and let $\{\mu_1, \cdots, \mu_l\}$ be the l shifts used in the LR-Smith(l) iteration. As stated in Section 3.2, (3.1) is equivalent to the Stein equation

$$\mathcal{P} - A_d \mathcal{P} A_d^T + B_d B_d^T = 0 \tag{4.1}$$

where A_d, and B_d are defined in (3.7) and (3.10) respectively. Then the k^{th} LR-Smith(l) iterate is simply given by (3.12):

$$Z_k^{Sl} = [\, B_d \;\; A_d B_d \;\; A_d^2 B_d \;\; \cdots \;\; A_d^{k-1} B_d \,].$$

Hence, the approximate low-rank gramian at the k^{th} step is

$$\mathcal{P}_k^{Sl} = Z_k^{Sl} (Z_k^{Sl})^T = \sum_{i=0}^{k-1} A_d^i B_d B_d^T (A_d^i)^T. \tag{4.2}$$

Let the short singular value decomposition (S-SVD hereafter) of Z_k^{Sl} be $Z_k^{Sl} = V \Sigma W^T$ where $V \in \mathbb{R}^{n \times (mlk)}$, $\Sigma \in \mathbb{R}^{(mlk)\times(mlk)}$, and $W \in \mathbb{R}^{(mlk)\times(mlk)}$. Then the S-SVD of $\mathcal{P}_k^{Sl}$ is given by $\mathcal{P}_k^{Sl} = V \Sigma^2 V^T$. Hence, it is enough to store only V and Σ. In other words, $\tilde{Z}_k = V\Sigma$ is also a low-rank square root factor for $\mathcal{P}_k^{Sl}$.

Let $\tau > 0$ be a pre-specified tolerance value. Assume that until the k^{th} step of the algorithm all the iterates $\mathcal{P}_i^{Sl}$ satisfy

$$\frac{\sigma_{min}(\mathcal{P}_i^{Sl})}{\sigma_{max}(\mathcal{P}_i^{Sl})} > \tau^2 \qquad \text{or equivalently} \qquad \frac{\sigma_{min}(Z_i^{Sl})}{\sigma_{max}(Z_i^{Sl})} = \frac{\sigma_{min}(\tilde{Z}_i)}{\sigma_{max}(\tilde{Z}_i)} > \tau \qquad \text{for } i = 1, 2, \cdots, k$$

where σ_{min} and σ_{max} denote the minimum and maximum singular values respectively. At the $(k+1)^{st}$ step, the approximants Z_{k+1}^{Sl} and $\mathcal{P}_{k+1}^{Sl}$ are readily computed as

$$Z_{k+1}^{Sl} = [Z_k^{Sl} \;\; A_d^k B_d] \quad \text{and} \quad \mathcal{P}_{k+1}^{Sl} = \mathcal{P}_k^{Sl} + A_d^k B_d B_d^T (A_d^k)^T.$$

Define $B_{(k)} = A_d^k B_d$ and decompose $B_{(k)}$ into the two spaces $Im(V)$ and $(Im(V))^{\perp}$; i.e. write

$$B_{(k)} = V\Gamma + \hat{V}\Theta. \tag{4.3}$$

where $\Gamma \in \mathbb{R}^{(mlk)\times(ml)}$, $\Theta \in \mathbb{R}^{(ml)\times(ml)}$, $V^T\hat{V} = 0$ and $\hat{V}^T\hat{V} = I_{ml}$. In view of (4.3), define the matrix

$$\hat{Z}_{k+1} = [\, V \;\; \hat{V} \,] \underbrace{\begin{bmatrix} \Sigma & \Gamma \\ 0 & \Theta \end{bmatrix}}_{\hat{S}} \tag{4.4}$$

Let $\hat{S}$ have the following SVD: $\hat{S} = T\hat{\Sigma}Y^T$. We note that since $\hat{S} \in \mathbb{R}^{(k+1)ml\times(k+1)ml}$, taking the SVD of $\hat{S}$ is inexpensive. It readily follows that $\tilde{Z}_{k+1}$ is given by

$$\tilde{Z}_{k+1} = \tilde{V}\hat{\Sigma} \qquad \text{where} \qquad \tilde{V} = [\, V \;\; \hat{V} \,]T, \tag{4.5}$$

where $\tilde{V} \in \mathbb{R}^{n\times(k+1)ml)}$ and $\hat{\Sigma} \in \mathbb{R}^{(k+1)ml\times(k+1)ml}$. Again one should notice that $\tilde{Z}_{k+1}$ is simply obtained by $\tilde{Z}_k$, which is already available, and the SVD of $\hat{S}$, which is easy to compute. Next, we partition $\hat{\Sigma}$ and $\tilde{V}$ conformably:

$$\tilde{Z}_{k+1} = [\, \tilde{V}_1 \;\; \tilde{V}_2 \,] \begin{bmatrix} \hat{\Sigma}_1 & \\ & \hat{\Sigma}_2 \end{bmatrix} \quad \text{so that} \quad \frac{\hat{\Sigma}_2(1,1)}{\hat{\Sigma}_1(1,1)} < \tau. \tag{4.6}$$

Then, the $(k+1)^{st}$ low-rank square root factor is approximated by

$$\tilde{Z}_{k+1} \approx \tilde{V}_1\hat{\Sigma}_1. \tag{4.7}$$

Indeed, we simply ignore the singular values, which are less than the given tolerance. Hence, while going from the k^{th} to the $(k+1)^{st}$ step, the number of columns of $\tilde{Z}_{k+1}$ generally does not increase. Indeed an increase will only occur if more than r singular values of $\tilde{Z}_{k+1}$ fall above the tolerance $\tau\sigma_1$. In any case, there can be at most ml additional columns added at any step which is the same as the unmodified LR-Smith(l) iteration discussed previously in Section 3.4. The case where $l = m = 1$ is worth mentioning: at each step, one column is added to $\tilde{Z}_k$, and by checking the condition $\frac{\sigma_{min}(\tilde{Z}_{k+1})}{\sigma_{max}(\tilde{Z}_{k+1})} < \tau$, we decide whether to keep the last singular vector and value or not.

Using $\tilde{Z}_{k+1}$, the $(k+1)^{st}$ step low-rank gramian is computed as

$$\tilde{\mathcal{P}}_{k+1} = \tilde{Z}_{k+1}(\tilde{Z}_{k+1})^T.$$

One should notice that the error between $\tilde{\mathcal{P}}_{k+1}$ and $\mathcal{P}_{k+1}^{Sl}$ is bounded by

$$\|E\| = \|\mathcal{P}_{k+1}^{Sl} - \tilde{\mathcal{P}}_{k+1}\| \leq (\sigma_{max}(\tilde{Z}_{k+1}))^2\tau^2,$$

Hence the error is in the order of $\mathcal{O}(\tau^2)$. If the above process is repeated q more steps and we obtain the iterates $\tilde{Z}_{k+q}$ and $\tilde{\mathcal{P}}_{k+q}$. The error $E_q = \mathcal{P}_{k+q}^{Sl} - \tilde{\mathcal{P}}_{k+q}$ satisfies

$$\|E_q\| = \|\mathcal{P}_{k+q}^{Sl} - \tilde{\mathcal{P}}_{k+q}\| \leq \tau^2 \sum_{i=1}^{q} (\sigma_{max}(\tilde{Z}_{k+i}))^2. \tag{4.8}$$

Once again the error is of order $\mathcal{O}(\tau^2)$.

4.2 Convergence Properties of the Modified LR-Smith(l) Iteration

In this section we present some convergence results for the k step approximate solutions $\tilde{\mathcal{P}}_k$ and $\tilde{\mathcal{Q}}_k$ which are, respectively, the modified LR-Smith(l) solutions to the two Lyapunov equations

$$A\mathcal{P} + \mathcal{P}A^{T} + BB^{T} = 0, \qquad A^{T}\mathcal{Q} + \mathcal{Q}A + C^{T}C = 0$$

where $A \in \mathbb{R}^{n\times n}$, $B \in \mathbb{R}^{n\times m}$, and $C \in \mathbb{R}^{p\times n}$. Before stating the results, we need some definitions:

Definition 4.1 *Let $\mathcal{I}_{\mathcal{P}}$ denote the set of indices i for which some columns have been eliminated from the i^{th} step approximant*

$$\mathcal{I}_{\mathcal{P}} = \{i : \text{such that in (4.6) } \hat{\Sigma}_2 \neq 0 \text{ for } \tilde{Z}_i,\ i = 1, 2, \cdots, k\}.$$

Then for each $i \in \mathcal{I}_{\mathcal{P}}$, let $n_i^{\mathcal{P}}$ denote the number of the neglected singular values. $\mathcal{I}_{\mathcal{Q}}$ and $n_i^{\mathcal{Q}}$ are defined similarly.

Proposition 4.1 *Let $\tilde{Z}_k$ be the k^{th} step modified LR-Smith(l) iterate corresponding to (4.1), $\tilde{\mathcal{P}}_k = \tilde{Z}_k(\tilde{Z}_k)^{T}$, and $\mathcal{P}_k^{Sl}$ be the k^{th} step LR-Smith(l) iterate given by (4.2). Define $\Delta_{kp} := \mathcal{P} - \tilde{\mathcal{P}}_k$. $\tilde{\mathcal{P}}_k$ and Δ_{kp} satisfy*

$$\|\Delta_{kp}\| = \|\mathcal{P}_k^{Sl} - \tilde{\mathcal{P}}_k\| \leq \tau^2 \sum_{i\in\mathcal{I}_{\mathcal{P}}} (\sigma_{max}(\tilde{Z}_i))^2, \tag{4.9}$$

$$0 \ \leq \ \mathbf{Tr}\,(\Delta_{kp}) = \mathbf{Tr}\,(\mathcal{P}_k^{Sl} - \tilde{\mathcal{P}}_k) \leq \tau^2 \sum_{i\in\mathcal{I}_{\mathcal{P}}} n_i^{\mathcal{P}} (\sigma_{max}(\tilde{Z}_i))^2, \tag{4.10}$$

where τ is the tolerance value of the modified LR-Smith(l) algorithm.

Proof: (4.9) is simply obtained from (4.8) using the definition of $\mathcal{I}_{\mathcal{P}}$. The lower bound for $\mathbf{Tr}\,(\Delta_{kp})$ in (4.10) is obvious. The upper bound for $\mathbf{Tr}\,(\Delta_{kp})$ readily follows by observing that

$$\mathbf{Tr}\,(\mathcal{P}_k^{Sl} - \tilde{\mathcal{P}}_k) = \sum_{i=1}^{k} \mathbf{Tr}\,(\mathcal{P}_i^{Sl} - \mathcal{P}_{i-1}^{Sl}) - \sum_{i=1}^{k} \mathbf{Tr}\,(\tilde{\mathcal{P}}_i - \tilde{\mathcal{P}}_{i-1}) + \mathcal{P}_0 - \tilde{\mathcal{P}}_0.$$

In view of Proposition 3.1, the following result holds:

Proposition 4.2 *Let $\tilde{Z}_k$ be the k^{th} step modified LR-Smith(l) iterate corresponding, to (4.1), $\tilde{\mathcal{P}}_k = \tilde{Z}_k(\tilde{Z}_k)^{T}$, $E_{kp} = \mathcal{P} - \tilde{\mathcal{P}}_k$. Let $A = X\Lambda X^{-1}$ be the eigenvalue decomposition of A. The k step modified LR-Smith(l) iterates satisfy*

$$0 \ \leq \ \mathbf{Tr}\,(E_{kp}) = \mathbf{Tr}\,(\mathcal{P} - \tilde{\mathcal{P}}_k) \leq K\,m\,l\,(\rho(A_d))^{2k}\mathbf{Tr}\,(\mathcal{P}) + \tau^2 \sum_{i\in\mathcal{I}_{\mathcal{P}}} n_i^{\mathcal{P}}\ (\sigma_{max}(\tilde{Z}_i))^2 \tag{4.11}$$

where K is given by (3.18).

Proof: The lower bound is again clear. To obtain the upper bound we proceed as follows: It follows from the definition $\mathcal{P}$, $\mathcal{P}_k^{Sl}$ and $\tilde{\mathcal{P}}_k$ that

$$\mathbf{Tr}\,(\mathcal{P} - \tilde{\mathcal{P}}_k) = \mathbf{Tr}\,(\mathcal{P} - \mathcal{P}_k^{Sl}) + \mathbf{Tr}\,(\mathcal{P}_k^{Sl} - \tilde{\mathcal{P}}_k). \tag{4.12}$$

Combining (4.12) and (4.10) with Proposition 3.1 leads to the desired result. ■

We note that the bounds for the traces of the errors in Proposition 3.1 and Proposition 4.2 differ only by an order of $\mathcal{O}(\tau^2)$. These bounds will be examined in more detail by means of numerical examples in Section 5.

The next results concerns the convergence of the computed Hankel singular values in a way analogous to Corollary 3.1.

Corollary 4.1 *Let σ_i and $\tilde{\sigma}_i$ denote Hankel singular values resulting from the full-rank exact gramians $\mathcal{P}$ and $\mathcal{Q}$ and from the modified LR-Smith(l) approximants $\tilde{\mathcal{P}}_k$ and $\tilde{\mathcal{Q}}_k$ respectively: ${\sigma_i}^2 = \lambda_i(\mathcal{P}\mathcal{Q})$ and $\tilde{\sigma}_i^2 = \lambda_i(\tilde{\mathcal{P}}_k\tilde{\mathcal{Q}}_k)$. Define $\hat{n} = kl\min(m,p)$. Then,*

$$\begin{aligned}0 \;\leq\; \sum_{i=1}^{n}\sigma_i^2 - \sum_{i=1}^{\hat{n}}\tilde{\sigma}_i^2 \;\leq\; & K\,l\,(\rho(A_d))^{2k}\Big(K\,\min(m,p)(\rho(A_d))^{2k}\mathbf{Tr}\,(P)\,\mathbf{Tr}\,(Q)+ \\ & m\,\mathbf{Tr}\,(\mathcal{P})\sum_{i=0}^{k-1}\|C_dA_d^j\|_2^2 + p\,\mathbf{Tr}\,(\mathcal{Q})\sum_{i=0}^{k-1}\|A_d^jB_d\|_2^2 + \\ & \tau_{\mathcal{P}}^2\|\mathcal{Q}_k^{Sl}\|\sum_{i\in\mathcal{I}_{\mathcal{P}}} n_i^{\mathcal{P}}\;(\sigma_{max}(\tilde{Z}_i))^2 + \tau_{\mathcal{Q}}^2\|\mathcal{P}_k^{Sl}\|\sum_{i\in\mathcal{I}_{\mathcal{Q}}} n_i^{\mathcal{Q}}\;(\sigma_{max}(\tilde{Y}_i))^2 + \\ & \tau_{\mathcal{P}}^2\tau_{\mathcal{Q}}^2\sum_{i\in\mathcal{I}_{\mathcal{P}}}(\sigma_{max}(\tilde{Z}_i))^2\sum_{i\in\mathcal{I}_{\mathcal{Q}}} n_i^{\mathcal{Q}}\;(\sigma_{max}(\tilde{Y}_i))^2\Big)\end{aligned} \tag{4.13}$$

where $\tau_{\mathcal{P}}$ and $\tau_{\mathcal{Q}}$ are the given tolerance values; and K is as defined in (3.18).

Proof: From the definitions of σ_i and $\tilde{\sigma}_i$ follows

$$\begin{aligned}\sum_{i=1}^{n}\sigma_i^2 - \sum_{i=1}^{\hat{n}}\tilde{\sigma}_i^2 &= \mathbf{Tr}\,(\mathcal{P}\mathcal{Q}) - \mathbf{Tr}\,(\tilde{\mathcal{P}}_k\tilde{\mathcal{Q}}_k) \\ &= \mathbf{Tr}\,(\mathcal{P}\mathcal{Q} - \mathcal{P}_k^{Sl}\mathcal{Q}_k^{Sl}) + \mathbf{Tr}\,(\mathcal{P}_k^{Sl}E_q) + \mathbf{Tr}\,(\mathcal{Q}_k^{Sl}E_p) - \mathbf{Tr}\,(E_pE_q)\end{aligned}$$

where $E_p = \mathcal{P}_k^{Sl} - \tilde{\mathcal{P}}_k$ and $E_q = \mathcal{Q}_k^{Sl} - \tilde{\mathcal{Q}}_k$. From Corollary 3.1, we know that $\mathbf{Tr}\,(\mathcal{P}\mathcal{Q} - \mathcal{P}_k^{Sl}\mathcal{Q}_k^{Sl}) \geq 0$. It is shown in [24] that for two $n \times n$ symmetric positive semidefinite matrices M and N, there holds $\lambda_n(M)\mathbf{Tr}\,(N) \leq \mathbf{Tr}\,(MN)$ where $\lambda_n(M)$ denotes the smallest eigenvalue of M. Hence we obtain $\mathbf{Tr}\,(\mathcal{Q}_k^{Sl}E_p) \geq \lambda_n(\mathcal{Q}_k^{Sl})\mathbf{Tr}\,(E_p) \geq 0$. Applying the same result to $\mathbf{Tr}\,(\mathcal{P}_k^{Sl}E_q - E_pE_q) = \mathbf{Tr}\,(\tilde{\mathcal{P}}E_q)$ where both $\tilde{\mathcal{P}} \geq 0$ and $E_q \geq 0$, we prove that $\mathbf{Tr}\,(\mathcal{P}_k^{Sl}E_q - E_pE_q) \geq 0$ and consequently $0 \leq \sum_{i=1}^{n}\sigma_i^2 - \sum_{i=1}^{\hat{n}}\tilde{\sigma}_i^2$. Using the relationships

$$\mathbf{Tr}\,(\mathcal{P}_k^{Sl}E_q) \leq \|\mathcal{P}_k^{Sl}\|\;\tau_{\mathcal{Q}}^2\sum_{i\in\mathcal{I}_{\mathcal{Q}}} n_i^{\mathcal{Q}}\;(\sigma_{max}(\tilde{Y}_i))^2 \tag{4.14}$$

$$\mathbf{Tr}\,(\mathcal{Q}_k^{Sl}E_p) \leq \|\mathcal{Q}_k^{Sl}\|\;\tau_{\mathcal{P}}^2\sum_{i\in\mathcal{I}_{\mathcal{P}}} n_i^{\mathcal{P}}\;(\sigma_{max}(\tilde{Z}_i))^2 \tag{4.15}$$

$$\mathbf{Tr}\,(E_pE_q) \leq \|E_p\|\mathbf{Tr}\,(E_q) \leq \tau_{\mathcal{P}}^2\tau_{\mathcal{Q}}^2\sum_{i\in\mathcal{I}_{\mathcal{P}}}(\sigma_{max}(\tilde{Z}_i))^2\sum_{i\in\mathcal{I}_{\mathcal{Q}}} n_i^{\mathcal{Q}}\;(\sigma_{max}(\tilde{Y}_i))^2 \tag{4.16}$$

together with Corollary 3.1 yields the desired result.

Once again the bounds for the error in the computed Hankel singular values in Corollary 3.1 and Corollary 4.1 differs only by the summation of terms in the order of $\mathcal{O}(\tau_{\mathcal{P}}^2)$, $\mathcal{O}(\tau_{\mathcal{Q}}^2)$, and $\mathcal{O}(\tau_{\mathcal{P}}^2\tau_{\mathcal{P}}^2)$. As will be illustrated in Section 5, these two upper bounds are very close.

4.3 A discussion of the approximately balanced reduced system

Let $\mathbf{\Sigma}_r = \left(\begin{array}{c|c} A_r & B_r \\ \hline C_r & D\end{array}\right) = \left(\begin{array}{c|c} W_r^TAV_r & W_r^TB \\ \hline CV_r & D\end{array}\right)$ be the r^{th} order reduced system obtained by exact balancing where W_r and V_r are given by (2.1). Similarly, let $\hat{\mathbf{\Sigma}}_r = \left(\begin{array}{c|c} \hat{A}_r & \hat{B}_r \\ \hline \hat{C}_r & D\end{array}\right) = \left(\begin{array}{c|c} \hat{W}_r^TA\hat{V}_r & \hat{W}_r^TB \\ \hline C\hat{V}_r & D\end{array}\right)$ be the r^{th} order reduced model obtained by approximate balancing where the approximate low-rank square-roots Z_k^{Sl} and Y_k^{Sl} are used instead of the exact square-roots in computing $\hat{W}_r$ and $\hat{V}_r$. The following equations are easily derived:

$$\hat{A}_r\hat{S}_r + \hat{S}_r\hat{A}_r^T + \hat{B}_r\hat{B}_r{}^T = \hat{W}_r^T(A\Delta + \Delta A^T)\hat{W}_r$$

where Δ is the error in $\mathcal{P}$, i.e. $\Delta = \mathcal{P} - \mathcal{P}_k^{Sl}$ and $\hat{S}_r$ is the diagonal matrix with the diagonal elements being the approximate Hankel singular values. It is clear that the stability of the reduced system is not always guaranteed. However, this does not seem to be a difficulty in practice; we obtained a stable reduced system for each of our computational examples.

Next we examine how close $\mathbf{\Sigma}_r$ is to $\hat{\mathbf{\Sigma}}_r$. To proceed towards this goal, define $\Delta_V := V_r - \hat{V}_r$ and $\Delta_W := W_r - \hat{W}_r$ and let $\|\Delta_V\| \leq \tau$ and $\|\Delta_W\| \leq \tau$ where τ is a small number; in other words we assume that $\hat{V}_r$ and $\hat{W}_r$ are close to V_r and W_r respectively. One may show that $\Delta_A := A_r - \hat{A}_r$, $\Delta_B := B_r - \hat{B}_r$ and $\Delta_C := C_r - \hat{C}_r$ satisfy

$$\|\Delta_A\| \leq \tau\|A\|(\|W_r\| + \|V_r\|) + \tau^2\|A\|, \qquad \|\Delta_B\| \leq \tau\|B_r\|, \qquad \text{and} \qquad \|\Delta_C\| \leq \tau\|C_r\|.$$

To simplify the discussion, we shall assume that $(jw - \hat{A}_r)^{-1} \approx (jw - A_r)^{-1} + \hat{\Delta}_A$ holds for every $w \in \mathbb{R}$ where $\hat{\Delta}_A$ satisfies the same upper bound as Δ_A, i.e. $\|\hat{\Delta}_A\| \leq \tau\|A\|(\|W_r\| + \|V_r\|) + \tau^2\|A\|$. Under these assumptions, one can show that

$$\|\mathbf{\Sigma}_r - \hat{\mathbf{\Sigma}}_r\|_\infty \leq \tau\left(\|C_r\|\,\|B_r\|\,\|A_r\|\,(\,\|W_r\| + \|V_r\|\,) + \|\mathbf{\Sigma}_1\|_\infty\|B_r\| + \|\mathbf{\Sigma}_2\|_\infty\|C_r\|\,\right) + \mathcal{O}(\tau^2) \tag{4.17}$$

where $\mathbf{\Sigma}_1 := \left(\begin{array}{c|c} A_r & I \\ \hline C_r & \end{array}\right)$ and $\mathbf{\Sigma}_2 := \left(\begin{array}{c|c} A_r & B_r \\ \hline I & \end{array}\right)$. Hence for small τ, i.e. when $\hat{V}_r$ and $\hat{W}_r$ are, respectively, close to V_r and W_r, we expect $\mathbf{\Sigma}_r$ to be close to $\hat{\mathbf{\Sigma}}_r$. Indeed as the examples below show, $\hat{\mathbf{\Sigma}}_r$ behaves much better than the above upper bound predicts.

5 Examples

This section illustrates the results by means of three numerical examples. In each example, both the LR-Smith(l) iterates $\mathcal{P}_k^{Sl}$, and $\mathcal{Q}_k^{Sl}$; and the modified LR-Smith(l) iterates $\tilde{\mathcal{P}}_k$, and $\tilde{\mathcal{Q}}_k$ are computed. The error bounds introduced in Section 4.2 are investigated. Also for both example, the balanced reduction is applied using the full rank gramians $\mathcal{P}$, $\mathcal{Q}$ and the approximate gramians $\mathcal{P}_k^{Sl}$, $\mathcal{Q}_k^{Sl}$; and $\tilde{\mathcal{P}}_k$, $\tilde{\mathcal{Q}}_k$. The resulting reduced order systems and Hankel Singular values are compared.

5.1 Example-1: CD Player

The full order model (FOM) describes the dynamics of a portable CD player and is of order 120, and single-input single-output. The eigenvalues of A have both very high and very low real and imaginary part, i.e. the eigenvalues are scattered in the complex plane. This makes it harder to obtain a low $\rho(A_d)$. A single shift results in $\rho(A_d) = 0.99985$. Indeed, even with a high number of multiple shifts, $l = 40$, $\rho(A_d)$ could not be reduced to less than 0.98. Hence only a single shift is considered. LR-Smith(l) and the modified LR-Smith(l) iterations are run for $k = 70$ iterations. The tolerance values are chosen to be $\tau_{\mathcal{P}} = 1 \times 10^{-6}$ for $\tilde{\mathcal{P}}_k$ and $\tau_{\mathcal{Q}} = 8 \times 10^{-6}$ for $\tilde{\mathcal{Q}}_k$. The resultant low rank LR-Smith(l) square root factors Z_k^{Sl} and Y_k^{Sl} has 70 columns. On the other hand the proposed algorithm yield low-rank square root factors $\tilde{Z}_k$ and $\tilde{Y}_k$ which have only 25 columns. The relative error between the computed gramians are

$$\frac{\|\mathcal{P}_k^{Sl} - \tilde{\mathcal{P}}_k\|}{\|\mathcal{P}_k^{Sl}\|} = 4.13 \times 10^{-10}, \text{ and } \qquad \frac{\|\mathcal{Q}_k^{Sl} - \tilde{\mathcal{Q}}_k\|}{\|\mathcal{Q}_k^{Sl}\|} = 2.33 \times 10^{-10}.$$

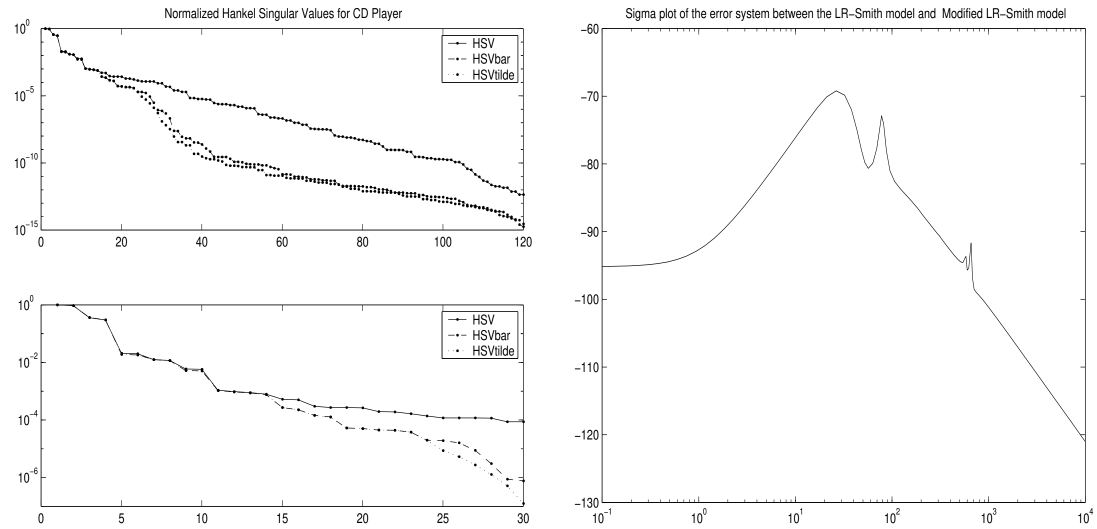

(a) (b)

Figure 1: (a) The normalized Hankel singular values σ_i's, $\hat{\sigma}_i$'s, and $\tilde{\sigma}_i$'s of CD example (b) The amplitude Bode plot of error system $\mathbf{\Sigma}_k^{Sl} - \tilde{\mathbf{\Sigma}}_k$ for CD example

These numbers proves the effectiveness of the proposed algorithm. Although the number of columns of the square root factor have been reduced almost 3 times, the computed gramians are very close to those obtained by LR-Smith(l) method. The errors between the exact and computed gramians are are obtained as

$$\frac{\|\mathcal{P} - \mathcal{P}_k^{Sl}\|}{\|\mathcal{P}\|} = \frac{\|\mathcal{P} - \tilde{\mathcal{P}}_k\|}{\|\mathcal{P}\|} = 3.95 \times 10^{-3}, \text{ and } \qquad \frac{\|\mathcal{Q} - \mathcal{Q}_k^{Sl}\|}{\|\mathcal{Q}\|} = \frac{\|\mathcal{Q} - \tilde{\mathcal{Q}}_k\|}{\|\mathcal{Q}\|} = 8.24 \times 10^{-1}.$$

Figure 1-(a) depicts the normalized[1] Hankel singular values (HSV) of the FOM, σ_i; HSV resulting from $\mathcal{P}_k^{Sl}$ and $\mathcal{Q}_k^{Sl}$, $\hat{\sigma}_i$; and HSV resulting from $\tilde{\mathcal{P}}_k$ and $\tilde{\mathcal{Q}}_k$, $\tilde{\sigma}_i$. As the figure shows, the largest 14 of $\hat{\sigma}_i$'s are very well approximated. Moreover the largest 25 of $\hat{\sigma}_i$'s are $\tilde{\sigma}_i$'s are almost equal, and some small deviations are observed after the 25^{th} one. The error between $\hat{\sigma}_i$'s and $\tilde{\sigma}_i$'s are

$$\sum \hat{\sigma}_i - \sum \tilde{\sigma}_i = 1.64 \times 10^{-3}.$$

All the errors and the corresponding error bounds are tabulated in Table 1. One should notice that the error bounds (4.9) for the norm and (4.10) for the trace are tight as expected. Recall that these errors are in the order of $\mathcal{O}(\tau^2)$. Also as stated after Corollary 4.1, the upper bounds for the errors in the computed HSV $\hat{\sigma}_i$'s and $\tilde{\sigma}_i$ are very close. The bounds (3.20) and (4.13) are pessimistic because of the slow convergence ($\rho(A_d) = 0.99985$) as stated in Remark 3.2. **However, what is important regarding the the proposed algorithm is the tightness of (4.9) and (4.10) and closeness of the upper bounds (3.20) and (4.13) which prove the effectiveness of the proposed method.**

After computing the approximate square root factors the balanced reduction is applied to the FOM using the approximate and the exact solutions; and the order is reduced to $r = 12$. Let $\mathbf{\Sigma}_k$, $\mathbf{\Sigma}_k^{Sl}$ and $\tilde{\mathbf{\Sigma}}_k$ denote the 12^{th} order reduced systems obtained through balanced reduction using the exact square root factors Z and Y; the LR-Smith(l) iterates Z_k^{Sl} and Y_k^{Sl}; and the the modified LR-Smith(l) iterates $\tilde{Z}_k$ and $\tilde{Y}_k$ respectively. Also let $\mathbf{\Sigma}$ denote the FOM. Figure 2-(a) depicts the amplitude Bode plots of the FOM $\mathbf{\Sigma}$ and the reduced systems $\mathbf{\Sigma}_k$, $\mathbf{\Sigma}_k^{Sl}$ and $\tilde{\mathbf{\Sigma}}_k$. As Figure 2-(a) shows, although the approximate gramians are not very good approximations of the exact gramians, $\mathbf{\Sigma}_k^{Sl}$ and $\tilde{\mathbf{\Sigma}}_k$ are very close to $\mathbf{\Sigma}_k$. The amplitude Bode plots of the error systems $\mathbf{\Sigma} - \mathbf{\Sigma}_k$, $\mathbf{\Sigma} - \mathbf{\Sigma}_k^{Sl}$

[1] For comparison, the highest Hankel singular value of each system is normalized to 1.

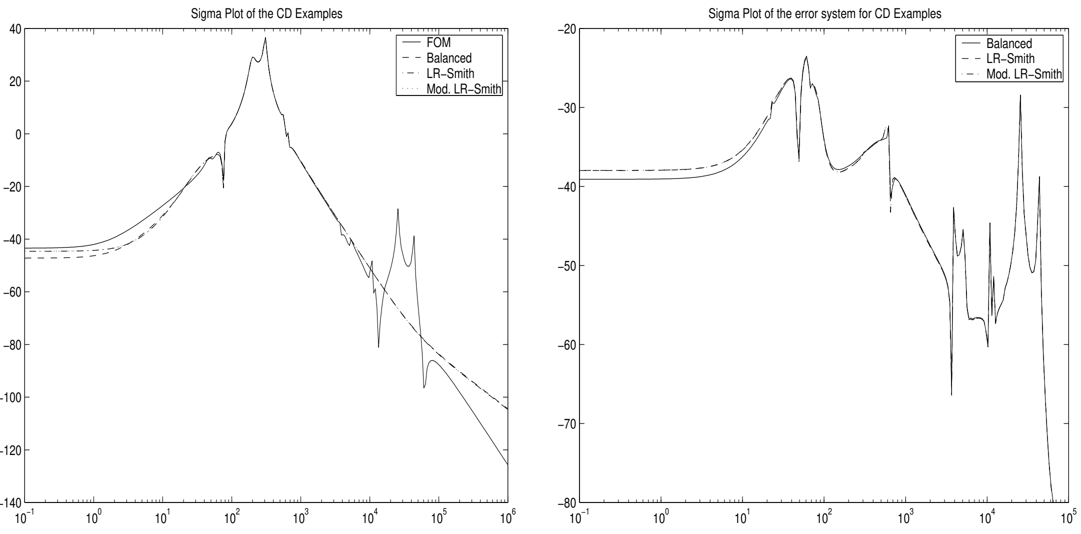

(a) (b)

Figure 2: (a) The amplitude Bode plots of the FOM $\mathbf{\Sigma}$ and the reduced systems $\mathbf{\Sigma}_k$, $\mathbf{\Sigma}_k^{Sl}$ and $\tilde{\mathbf{\Sigma}}_k$ (b) the amplitude Bode plots of error systems $\mathbf{\Sigma} - \mathbf{\Sigma}_k$, $\mathbf{\Sigma} - \mathbf{\Sigma}_k^{Sl}$ and $\mathbf{\Sigma} - \tilde{\mathbf{\Sigma}}_k$ for CD Example

and $\mathbf{\Sigma} - \tilde{\mathbf{\Sigma}}_k$ are illustrated in Figure 2-(b). We note that $\mathbf{\Sigma}_k^{Sl}$ and $\tilde{\mathbf{\Sigma}}_k$ are almost equal as expected since the errors between $\tilde{\mathcal{P}}_k$ and $\mathcal{P}_k^{Sl}$, and $\tilde{\mathcal{Q}}_k$ and $\mathcal{Q}_k^{Sl}$ are very small, see Figure 1-(b). The relative[2] $\mathcal{H}_\infty$ norms of the error systems are tabulated in Table 1.

5.2 Example-2: Module-1r of the International Space Station

This is a model of component 1r (Russian service module) of the International Space Station. It has 270 states, 3 inputs and 3 outputs. As in Example-1, even with a high number of multiple shifts, $l = 20$, $\rho(A_d)$ could not be reduced to less than 0.9973. Hence again only a single shift is considered. We run the LR-Smith(l) and the modified LR-Smith(l) iterations for $k = 70$ iterations. The tolerance values are taken to to be $\tau_{\mathcal{P}} = 1 \times 10^{-4}$ for $\tilde{\mathcal{P}}_k$ and $\tau_{\mathcal{Q}} = 7 \times 10^{-5}$ for $\tilde{\mathcal{Q}}_k$. The resultant low rank LR-Smith(l) square root factors Z_k^{Sl} and Y_k^{Sl} has 210 columns. Recall that FOM has order 270. On the other hand the proposed algorithm yields low-rank square root factors $\tilde{Z}_k$ and $\tilde{Y}_k$ which have 106 columns. The relative error between the computed gramians are

$$\frac{\|\mathcal{P}_k^{Sl} - \tilde{\mathcal{P}}_k\|}{\|\mathcal{P}_k^{Sl}\|} = 4.59 \times 10^{-8}, \text{ and } \qquad \frac{\|\mathcal{Q}_k^{Sl} - \tilde{\mathcal{Q}}_k\|}{\|\mathcal{Q}_k^{Sl}\|} = 2.18 \times 10^{-8}.$$

As in the CD example, the proposed method works quite well. Although the number of columns of the square root factor have been reduced to half, again the computed gramians are very close to those obtained by LR-Smith(l) method. We compute the errors between the exact and computed gramians as well:

$$\frac{\|\mathcal{P} - \mathcal{P}_k^{Sl}\|}{\|\mathcal{P}\|} = \frac{\|\mathcal{P} - \tilde{\mathcal{P}}_k\|}{\|\mathcal{P}\|} = 8.40 \times 10^{-1}, \text{ and } \qquad \frac{\|\mathcal{Q} - \mathcal{Q}_k^{Sl}\|}{\|\mathcal{Q}\|} = \frac{\|\mathcal{Q} - \tilde{\mathcal{Q}}_k\|}{\|\mathcal{Q}\|} = 7.97 \times 10^{-1}.$$

The normalized σ_i's, $\hat{\sigma}_i$'s and $\tilde{\sigma}_i$'s are shown in Figure 3-(a). As the figure illustrates $\tilde{\sigma}_i$'s matches the $\hat{\sigma}_i$'s quite well. Indeed, the error between $\hat{\sigma}_i$'s and $\tilde{\sigma}_i$'s are

$$\sum \hat{\sigma}_i - \sum \tilde{\sigma}_i = 6.31 \times 10^{-7}.$$

[2]To find the relative error, we divide the norm of the error system with the corresponding norm of the full order system

$\|\mathcal{P}_k^{Sl} - \tilde{\mathcal{P}}_k\|$	upper bound	$\mathbf{Tr}\,(\mathcal{P}_k^{Sl} - \tilde{\mathcal{P}}_k)$	upper bound	$\sum \sigma_i^2 - \sum \hat{\sigma}_i^2$	upper bound
7.24×10^{-7}	6.27×10^{-6}	2.51×10^{-6}	6.27×10^{-6}	1.80×10^{1}	1.78×10^{10}

$\|\mathcal{Q}_k^{Sl} - \tilde{\mathcal{Q}}_k\|$	upper bound	$\mathbf{Tr}\,(\mathcal{Q}_k^{Sl} - \tilde{\mathcal{Q}}_k)$	upper bound	$\sum \sigma_i^2 - \sum \tilde{\sigma}_i^2$	upper bound
4.92×10^{-5}	3.68×10^{-4}	1.62×10^{-4}	3.68×10^{-4}	1.80×10^{1}	$1.78 \times 10^{10} + 1.9657$

$\|\mathbf{\Sigma} - \mathbf{\Sigma}_k\|_\infty$	$\|\mathbf{\Sigma} - \mathbf{\Sigma}_k^{Sl}\|_\infty$	$\|\mathbf{\Sigma} - \tilde{\mathbf{\Sigma}}_k\|_\infty$	$\|\mathbf{\Sigma}_k^{Sl} - \tilde{\mathbf{\Sigma}}_k\|_\infty$	$\|\mathbf{\Sigma}_k - \mathbf{\Sigma}_k^{Sl}\|_\infty$	$\|\mathbf{\Sigma}_k - \tilde{\mathbf{\Sigma}}_k\|_\infty$
9.88×10^{-4}	9.71×10^{-4}	9.69×10^{-4}	5.11×10^{-6}	1.47×10^{-4}	1.47×10^{-4}

Table 1: Numerical Results for Example-1

All the errors and the corresponding error bounds are tabulated in Table 2. The error bounds (4.9) and (4.10) are again tight. Also the upper bounds for the errors in the computed HSV $\hat{\sigma}_i$'s and $\tilde{\sigma}_i$ are almost equal. Due to the slow convergence and the non-normality of A matrix, as in the CD example, the bounds (3.20) and (4.13) are pessimistic.

We apply the balanced reduction FOM using the approximate and the exact solutions; and reduce the order to $r = 26$. Figure 4-(a) depicts the amplitude Bode plots of the FOM $\mathbf{\Sigma}$ and the reduced systems $\mathbf{\Sigma}_k$, $\mathbf{\Sigma}_k^{Sl}$ and $\tilde{\mathbf{\Sigma}}_k$. As seen from Figure 4-(a), although the approximate gramians are not good approximations of the exact gramians, $\mathbf{\Sigma}_k^{Sl}$ and $\tilde{\mathbf{\Sigma}}_k$ are very close to $\mathbf{\Sigma}_k$. All the reduced models match the FOM quite well. The amplitude Bode plots of the error systems $\mathbf{\Sigma} - \mathbf{\Sigma}_k$, $\mathbf{\Sigma} - \mathbf{\Sigma}_k^{Sl}$ and $\mathbf{\Sigma} - \tilde{\mathbf{\Sigma}}_k$ are illustrated in Figure 4-(b). Again $\mathbf{\Sigma}_k^{Sl}$ and $\tilde{\mathbf{\Sigma}}_k$ are almost identical, see Figure 3-(b) which shows the Bode plots of the error $\mathbf{\Sigma}_k^{Sl} - \tilde{\mathbf{\Sigma}}_k$. The relative $\mathcal{H}_\infty$ norms of the error systems are tabulated in Table 2.

$\|\mathcal{P}_k^{Sl} - \tilde{\mathcal{P}}_k\|$	upper bound	$\mathbf{Tr}\,(\mathcal{P}_k^{Sl} - \tilde{\mathcal{P}}_k)$	upper bound	$\sum \sigma_i^2 - \sum \hat{\sigma}_i^2$	upper bound
2.04×10^{-7}	1.45×10^{-6}	1.38×10^{-6}	3.29×10^{-6}	$7.23. \times 10^{-3}$	1.62×10^{8}

$\|\mathcal{Q}_k^{Sl} - \tilde{\mathcal{Q}}_k\|$	upper bound	$\mathbf{Tr}\,(\mathcal{Q}_k^{Sl} - \tilde{\mathcal{Q}}_k)$	upper bound	$\sum \sigma_i^2 - \sum \tilde{\sigma}_i^2$	upper bound
9.69×10^{-11}	7.11×10^{-7}	6.91×10^{-10}	1.57×10^{-6}	7.23×10^{-3}	$1.62 \times 10^{8} + 7.01 \times 10^{-6}$

$\|\mathbf{\Sigma} - \mathbf{\Sigma}_k\|_\infty$	$\|\mathbf{\Sigma} - \mathbf{\Sigma}_k^{Sl}\|_\infty$	$\|\mathbf{\Sigma} - \tilde{\mathbf{\Sigma}}_k\|_\infty$	$\|\mathbf{\Sigma}_k^{Sl} - \tilde{\mathbf{\Sigma}}_k\|_\infty$	$\|\mathbf{\Sigma}_k - \mathbf{\Sigma}_k^{Sl}\|_\infty$	$\|\mathbf{\Sigma}_k - \tilde{\mathbf{\Sigma}}_k\|_\infty$
2.89×10^{-3}	2.61×10^{-2}	2.61×10^{-2}	2.11×10^{-5}	3.03×10^{-2}	3.03×10^{-2}

Table 2: Numerical Results for Example-2

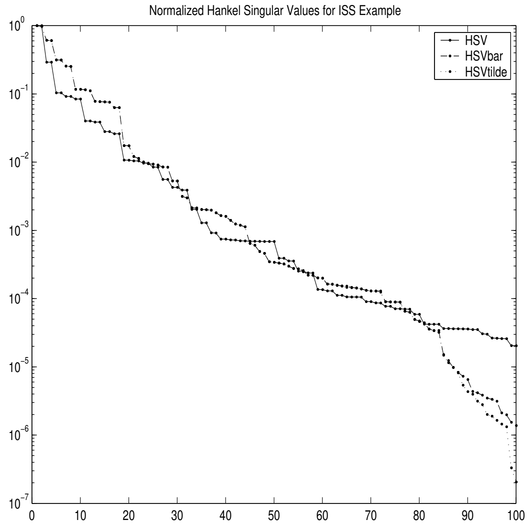

(a)

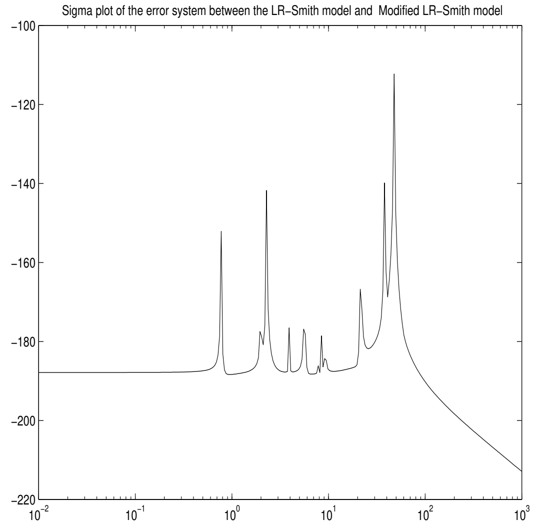

(b)

Figure 3: (a) The normalized Hankel singular values σ_i's, $\hat{\sigma}_i$'s, and $\tilde{\sigma}_i$'s of Module 1r (b) The amplitude Bode plot of error system $\mathbf{\Sigma}_k^{Sl} - \tilde{\mathbf{\Sigma}}_k$ for Module 1r

5.3 Example-3

This example is from [20]. The FOM is a dynamical system of order 1006. The state-space matrices are given by

$$A = \begin{bmatrix} A_1 & & & \\ & A_2 & & \\ & & A_3 & \\ & & & A_4 \end{bmatrix} \quad A_1 = \begin{bmatrix} -1 & 100 \\ -100 & -1 \end{bmatrix} \quad A_2 = \begin{bmatrix} -1 & 200 \\ -200 & -1 \end{bmatrix} \quad A_3 = \begin{bmatrix} -1 & 400 \\ -400 & -1 \end{bmatrix}$$

$$A_4 = diag(-1, \cdots, -1000), \;\; B^T = C = [\;\underbrace{10\;\cdots\;10}_{6}\;\;\underbrace{1\;\cdots 1}_{1000}]$$

$l = 10$ cyclic shifts are used, and $\rho(A_d)$ is reduced to 0.7623 which results in a fast convergence. It is easy to see that the spectrum of A is $\sigma(A) = \{-1, -2, \cdots, -1000, -1 \pm j100, -1 \pm j200, -1 \pm j400\}$. The 6 of the shifts are chosen so that the 6 complex eigenvalues of A are eliminated. We run the LR-Smith(l) and the modified LR-Smith(l) iterations for $k = 30$ iterations. The tolerance values are taken to to be $\tau_{\mathcal{P}} = \tau_{\mathcal{Q}} = 3 \times 10^{-5}$. The resultant low rank LR-Smith(l) square root factors Z_k^{Sl} and Y_k^{Sl} has 300 columns. On the other hand the proposed algorithm significantly reduces the number of columns and yields low-rank square root factors $\tilde{Z}_k$ and $\tilde{Y}_k$ which have only 19 columns. Although the number of columns has been much less than the one resulting from LR-Smith(l) method, the relative error between the computed gramians are very low; i.e. $\tilde{\mathcal{P}}_k$ and $\mathcal{P}_k^{Sl}$ are very close to each other:

$$\frac{\|\mathcal{P}_k^{Sl} - \tilde{\mathcal{P}}_k\|}{\|\mathcal{P}_k^{Sl}\|} = 1.90 \times 10^{-8}, \text{ and } \qquad \frac{\|\mathcal{Q}_k^{Sl} - \tilde{\mathcal{Q}}_k\|}{\|\mathcal{Q}_k^{Sl}\|} = 3.22 \times 10^{-8}.$$

These numbers once more prove the effectiveness of the algorithm. The errors between the exact and computed gramians are:

$$\frac{\|\mathcal{P} - \mathcal{P}_k^{Sl}\|}{\|\mathcal{P}\|} = 4.98 \times 10^{-10}, \qquad \frac{\|\mathcal{P} - \tilde{\mathcal{P}}_k\|}{\|\mathcal{P}\|} = 1.88 \times 10^{-8}$$

$$\frac{\|\mathcal{Q} - \mathcal{Q}_k^{Sl}\|}{\|\mathcal{Q}\|} = 4.98 \times 10^{-10}, \qquad \frac{\|\mathcal{Q} - \tilde{\mathcal{Q}}_k\|}{\|\mathcal{Q}\|} = 3.21 \times 10^{-8}.$$

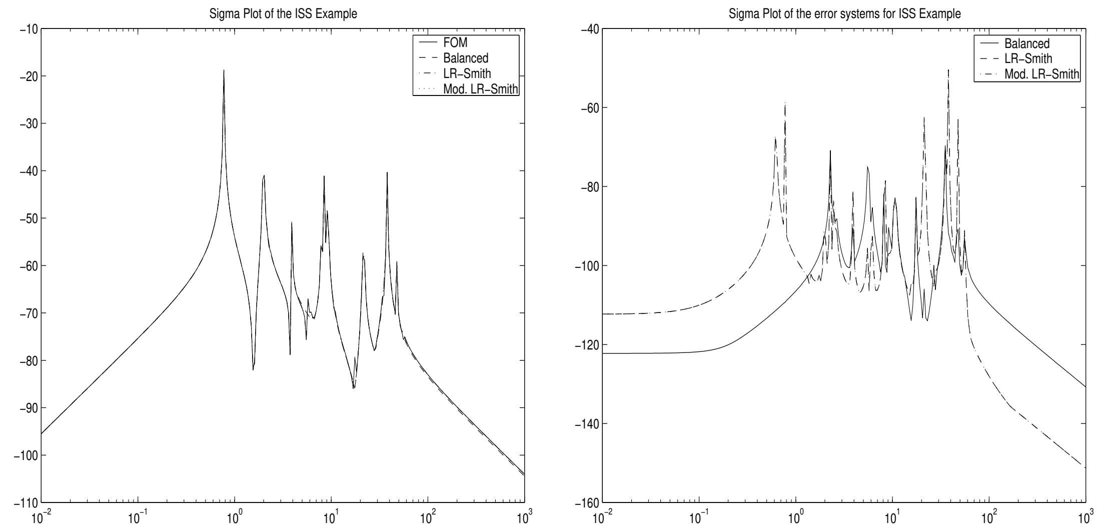

(a) (b)

Figure 4: (a) The amplitude Bode plots of the FOM $\mathbf{\Sigma}$ and the reduced systems $\mathbf{\Sigma}_k$, $\mathbf{\Sigma}_k^{Sl}$ and $\tilde{\mathbf{\Sigma}}_k$ (b) the amplitude Bode plots of error systems $\mathbf{\Sigma} - \mathbf{\Sigma}_k$, $\mathbf{\Sigma} - \mathbf{\Sigma}_k^{Sl}$ and $\mathbf{\Sigma} - \tilde{\mathbf{\Sigma}}_k$ for Module 1r

The first 19 normalized HSV's σ_i's, $\hat{\sigma}_i$'s and $\tilde{\sigma}_i$'s are depicted in Figure 5-(a). As seen from the figure, $\hat{\sigma}_i$'s and $\tilde{\sigma}_i$'s matches σ_i's quite well. Also, $\tilde{\sigma}_i$'s are almost equivalent to $\hat{\sigma}_i$'s. The error between $\hat{\sigma}_i$'s and $\tilde{\sigma}_i$'s are

$$\sum \hat{\sigma}_i - \sum \tilde{\sigma}_i = 2.76 \times 10^{-6}.$$

All the errors and the corresponding error bounds are tabulated in Table 3. As in the previous examples, the error bounds (4.9) and (4.10) are again tight. Also, the bounds (3.20) and (4.13) for the errors in are much tighter compared to the CD and ISS example. This results from the normality of A, and fast convergence rate, i.e. small $\rho(A_d)$.

$\|\mathcal{P}_k^{Sl} - \tilde{\mathcal{P}}_k\|$	upper bound	$\mathbf{Tr}\,(\mathcal{P}_k^{Sl} - \tilde{\mathcal{P}}_k)$	upper bound	$\sum \sigma_i^2 - \sum \hat{\sigma}_i^2$	upper bound
9.84×10^{-7}	1.35×10^{-6}	2.19×10^{-6}	1.30×10^{-5}	$2.99. \times 10^{-8}$	2.69×10^{-2}

$\|\mathcal{Q}_k^{Sl} - \tilde{\mathcal{Q}}_k\|$	upper bound	$\mathbf{Tr}\,(\mathcal{Q}_k^{Sl} - \tilde{\mathcal{Q}}_k)$	upper bound	$\sum \sigma_i^2 - \sum \tilde{\sigma}_i^2$	upper bound
8.60×10^{-7}	1.35×10^{-6}	2.68×10^{-6}	1.30×10^{-5}	5.02×10^{-6}	$2.69 \times 10^{-2} + 1.33 \times 10^{-3}$

$\|\mathbf{\Sigma} - \mathbf{\Sigma}_k\|_\infty$	$\|\mathbf{\Sigma} - \mathbf{\Sigma}_k^{Sl}\|_\infty$	$\|\mathbf{\Sigma} - \tilde{\mathbf{\Sigma}}_k\|_\infty$	$\|\mathbf{\Sigma}_k^{Sl} - \tilde{\mathbf{\Sigma}}_k\|_\infty$	$\|\mathbf{\Sigma}_k - \mathbf{\Sigma}_k^{Sl}\|_\infty$	$\|\mathbf{\Sigma}_k - \tilde{\mathbf{\Sigma}}_k\|_\infty$
1.47×10^{-4}	1.47×10^{-4}	1.47×10^{-4}	2.40×10^{-9}	7.25×10^{-11}	7.25×10^{-11}

Table 3: Numerical Results for Example-3

Using balanced reduction, a reduced model of order $r = 11$ is obtained. Figure 6-(a) depicts the amplitude Bode plots of the FOM $\mathbf{\Sigma}$ and the reduced systems $\mathbf{\Sigma}_k$, $\mathbf{\Sigma}_k^{Sl}$ and $\tilde{\mathbf{\Sigma}}_k$. As Figure 6-(a) illustrates, all the reduced

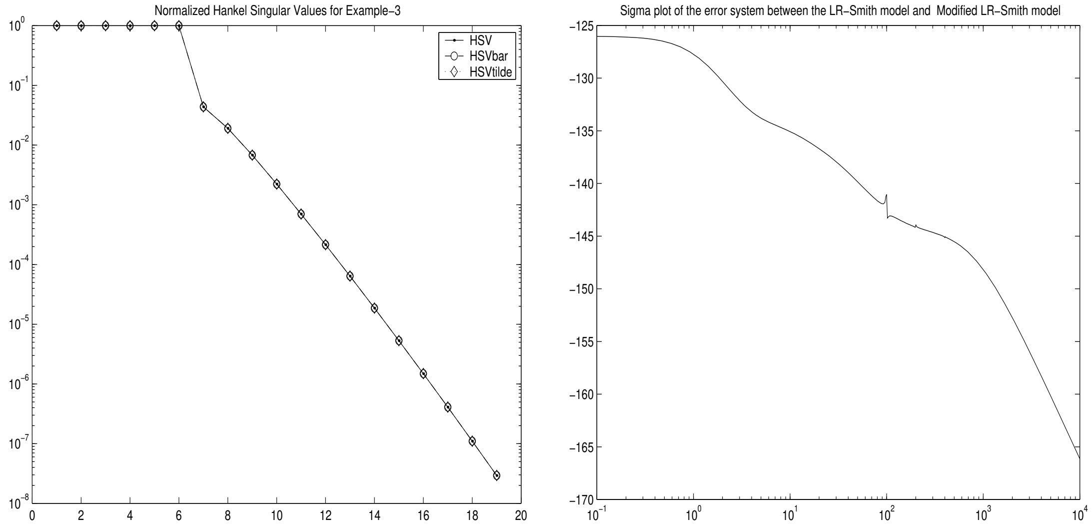

(a) (b)

Figure 5: (a) The normalized Hankel singular values σ_i's, $\hat{\sigma}_i$'s, and $\tilde{\sigma}_i$'s (b) The amplitude Bode plot of error system $\mathbf{\Sigma}_k^{Sl} - \tilde{\mathbf{\Sigma}}_k$ for Example-3

models match the FOM quite well. Also $\mathbf{\Sigma}_k^{Sl}$ and $\tilde{\mathbf{\Sigma}}_k$ are almost the same as $\mathbf{\Sigma}_k$, see the error norms in Table 3. The amplitude Bode plots of the error systems $\mathbf{\Sigma} - \mathbf{\Sigma}_k$, $\mathbf{\Sigma} - \mathbf{\Sigma}_k^{Sl}$ and $\mathbf{\Sigma} - \tilde{\mathbf{\Sigma}}_k$ are illustrated in Figure 6-(b). As in the previous 2 examples, $\mathbf{\Sigma}_k^{Sl}$ and $\tilde{\mathbf{\Sigma}}_k$ are almost identical. The relative $\mathcal{H}_\infty$ norm of the error $\mathbf{\Sigma}_k^{Sl} - \tilde{\mathbf{\Sigma}}_k$ is in the order of $\mathcal{O}(10^{-9})$, see also Figure 5-(b) which shows the Bode plots of the error $\mathbf{\Sigma}_k^{Sl} - \tilde{\mathbf{\Sigma}}_k$. Recall that $\mathbf{\Sigma}_k^{Sl}$ has been obtained using a square root factor of 300 columns, on the other hand $\tilde{\mathbf{\Sigma}}_k$ has been obtained using a square root factor of only 19 columns. This example proves that in case of multiple shift, the LR-Smith(l) iterate will include too much redundancy in the approximate solutions and give rise to memory problems. All the relative $\mathcal{H}_\infty$ norms of the error systems are tabulated in Table 3.

5.4 Example-4: Heat Distribution on a Plate

The FOM model describes the 2-dimensional heat equation on a square plate with adiabatic (no heat flux through the walls) boundary conditions. The plate consists of 9 sub-plates. The number of discretization points on both x and y axes are 144 which leads to a FOM of order 20736. Each sub-block is uniformly heated which results in $m = 9$ inputs. As observations, we choose the middle points of the each sub-blocks. This leads to $p = 9$ outputs. We run the proposed algorithm with tolerance values $\tau_{\mathcal{P}} = \tau_{\mathcal{Q}} = 10^{-6}$ for $k = 40$ steps using $l = 2$ shifts and obtain the low-rank square root factors $\tilde{Z}_k$ and $\tilde{Y}_k$ which have only 85 columns. Note that an exact LR-Smith(l) would have 720 columns. Using the approximate Cholesky factors $\tilde{Z}_k$ and $\tilde{Y}_k$ we apply the balanced reduction and reduce the order to $r = 9$. The reduced model is *almost* balanced as the following numerical results show where $\mathcal{P}_{red}$ and $\mathcal{Q}_{red}$ denote the gramians for the reduced model.

$$\|\mathcal{P}_{red} - \mathrm{diag}(\mathcal{P}_{red})\| = 7.28 \times 10^{-9}, \;\; \|\mathcal{Q}_{red} - \mathrm{diag}(\mathcal{Q}_{red})\| = 1.05 \times 10^{-12}, \;\; \|\mathcal{P}_{red} - \mathcal{Q}_{red}\| = 1.04 \times 10^{-9}.$$

Balancing a FOM of order 20736 with Cholesky factors having only 85 columns proves the effectiveness of the method. The sigma plots of the FOM and ROM, and that of the error model are shown in Figure 7-a and Figure 7-a respectively.

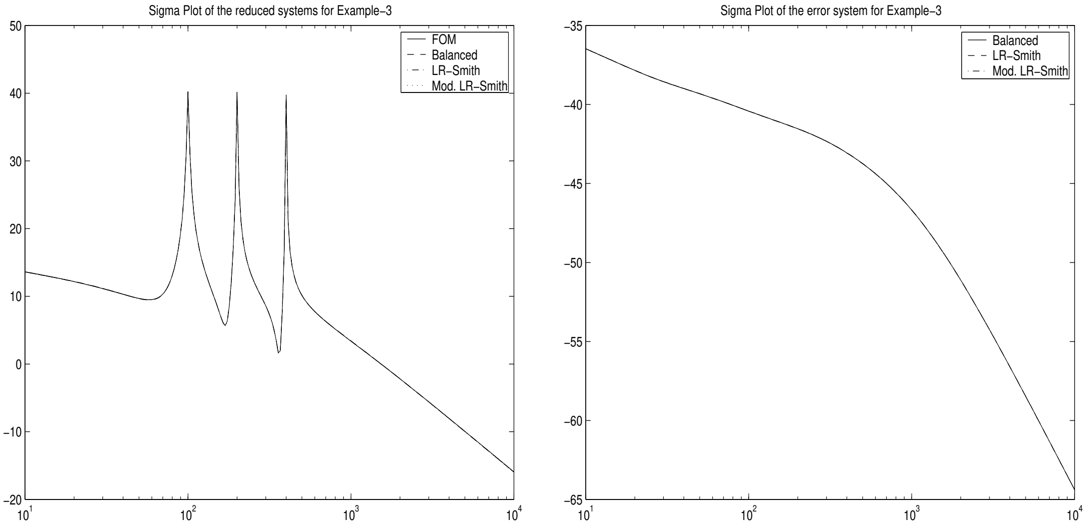

(a) (b)

Figure 6: (a) The amplitude Bode plots of the FOM $\mathbf{\Sigma}$ and the reduced systems $\mathbf{\Sigma}_k$, $\mathbf{\Sigma}_k^{Sl}$ and $\tilde{\mathbf{\Sigma}}_k$ (b) the amplitude Bode plots of error systems $\mathbf{\Sigma} - \mathbf{\Sigma}_k$, $\mathbf{\Sigma} - \mathbf{\Sigma}_k^{Sl}$ and $\mathbf{\Sigma} - \tilde{\mathbf{\Sigma}}_k$ for Example-3

6 Conclusions

We have presented a modified Cyclic Low-Rank Smith Method to compute the low-rank approximants to the solution of Lyapunov equations arising from large-scale dynamical systems. Unlike the original cyclic low-rank Smith Method, the number of the columns of the approximants do not necessarily increase at each step and, in the worst case, the increase in number is equal to the increase in cyclic low-rank Smith Method. We have demonstrated how to implement this method without having to store multiple factorizations of the shifted matrices. Moreover, we have established upper bounds for the errors in the low-rank approximants and in the resulting approximate Hankel singular values. These results are supported with four numerical examples that demonstrate the efficiency of the and accuracy algorithm.

References

[1] A.C. Antoulas, *Lectures on the approximation of linear dynamical systems*, Draft, to appear, SIAM Press 2002.

[2] A.C. Antoulas and D.C. Sorensen, *Projection methods for balanced model reduction*, Technical Report ECE-CAAM Depts, Rice University, March 2001.

[3] A.C. Antoulas, D.C. Sorensen, and S. Gugercin, *A survey of model reduction methods for large-scale systems*, Structured Matrices in Operator Theory, Numerical Analysis, Control, Signal and Image Processing, Contemporary Mathematics, AMS publications, 2001.

[4] A.C. Antoulas, D.C. Sorensen, and Y.K. Zhou, *On the decay rate of Hankel singular values and related issues*, to appear in Systems and Control Letters, 2002.

[5] R. H. Bartels and G. W. Stewart, *Solution of the matrix equation $AX + XA = C$: Algorithm 432*, Comm. ACM, 15: 820-826, 1972.

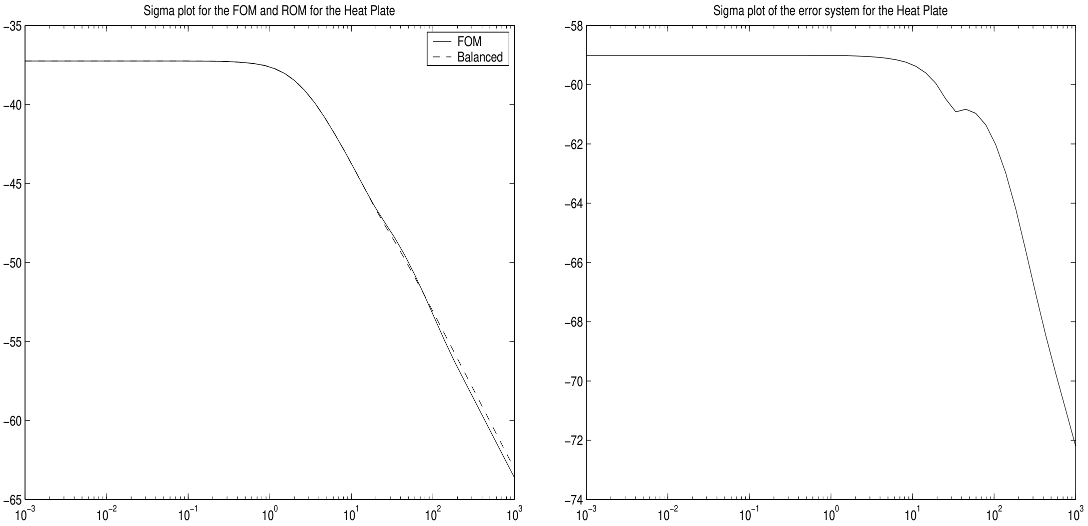

(a) (b)

Figure 7: (a) The amplitude Bode plots of the FOM and ROM (b) the amplitude Bode plots of error systems for Heat Example

[6] N. Ellner and E. Wachspress, *Alternating direction implicit iteration for systems with complex spectra*, SIAM J. Numer. Anal., 28: 859-870, 1991.

[7] K. Glover, *All optimal Hankel-norm approximations of linear multivariable systems and their L^∞-error bounds*, International Journal of Control, **39**: 1115-1193 (1984).

[8] G. H. Golub and C. F. Van Loan, *Matrix Computations*, John Hopkins University Press, Baltimore, Third Edition, 1996.

[9] S. Gugercin and A.C. Antoulas, *A comparative of 7 algorithms for model reduction*, in the Proceedings of 39^{th} CDC, Sydney, Australia, December 2000.

[10] S. Gugercin and A. C. Antoulas *Approximation of the International Space Station 1R and 12A models*, in the Proceedings of the 40^{th} CDC, December 2001.

[11] S. Hammarling, *Numerical solution of the stable, non-negative definite Lyapunov equation*, IMA J. Numer. Anal., 2, pp: 303-323, 1982.

[12] A. S. Hodel, K.P. Poola, and B. Tenison. *Numerical solution of the Lyapunov equation by approximate power iteration*, Linear Algebra Appl., 236: 205-230, 1996.

[13] D. Y. Hu and L. Reichel, *Krylov subspace methods for the Sylvester equation*, Linear Algebra Appl., 172: 283-313, 1992.

[14] I. M. Jaimoukha and E. M. Kasenally, *Krylov subspace methods for solving large Lyapunov equations*, SIAM J. Numerical Anal., 31: 227:251, 1994.

[15] B. C. Moore, *Principal Component Analysis in Linear System: Controllability, Observability and Model Reduction*, IEEE Transactions on Automatic Control, AC-26:17-32, 1981.

[16] A. Lu and E. L. Wachspress, *Solution of Lyapunov equations by alternating direction implicit iteration*, Computers Math. Appl., 21(9):43-58, 1991.

[17] D. W. Peaceman and H. H. Rachford, *The numerical solutions of parabolic and elliptic differential equations*, J. SIAM, 3: 28-41,, 1955.

[18] T. Penzl, *Eigenvalue Decay Bounds for Solutions of Lyapunov Equations: The Symmetric Case*, Systems and Control Letters, **40**: 139-144 (2000).

[19] T. Penzl, *A cyclic low-rank Smith method for large sparse Lyapunov equations*, SIAM J. Sci. Comput., Vol. 21, No. 4, pp: 1401-1418, 2000.

[20] T. Penzl, *Algorithms for model reduction of large dynamical systems*, Technical Report SFB393/99-40, Sonderforschungsbereich 393 Numerische Simulation auf massiv parallelen Rechern, TU Chemnitz, 09107, FRG, 1999. Available from `http://www.tu-chemnitz.de/sfb393/sfb99pr.html`.

[21] J. D. Roberts, *Linear model reduction and solution of the algebraic Riccati equation by use of the sign function*, International Journal of Control, 32: 677-687, 1980.

[22] G. Starke, *Optimal alternating direction implicit parameters for nonsymmetric systems of linear equations*, SIAM J. Numer. Anal., 28: 129-141, 1991.

[23] R. A. Smith, *Matrix Equation,* $XA + BX = C$, SIAM J. Appl. Math, 16: 198-201, 1968.

[24] W. Xing, Q. Zhang and Q. Wang, *A trace bound for a general square matrix product*, IEEE Transactions on Automatic Control, Vol. 45, No. 8, pp: 1563-1565, 2000.

[25] E. Wachspress, *Iterative solution of the Lyapunov matrix equation*, Appl. Math. Let., 1: 87-90, 1988.

[26] E. Wachspress, *The ADI minimax problem for complex spectra*, in Iterative Methods for Large Linear Systems, D. Kincaid and L. Hayes, edss, Academic Press, San Diego, pp: 251-271, 1990.